

Synthesis, Photophysical and Electrochemical Properties of Novel and Highly
Fluorescent Difluoroboron Flavanone β -Diketonate Complexes

Elida Betania Ariza Paez^a, Sergio Curcio^b, Natália P. Neme^{bc}, Matheus J.S. Matos^b, Rodrigo S. Correa^a, Fabio Junio Pereira^a, Flaviane Francisco Hilário^a, Thiago Cazati^b and Jason Guy Taylor^a

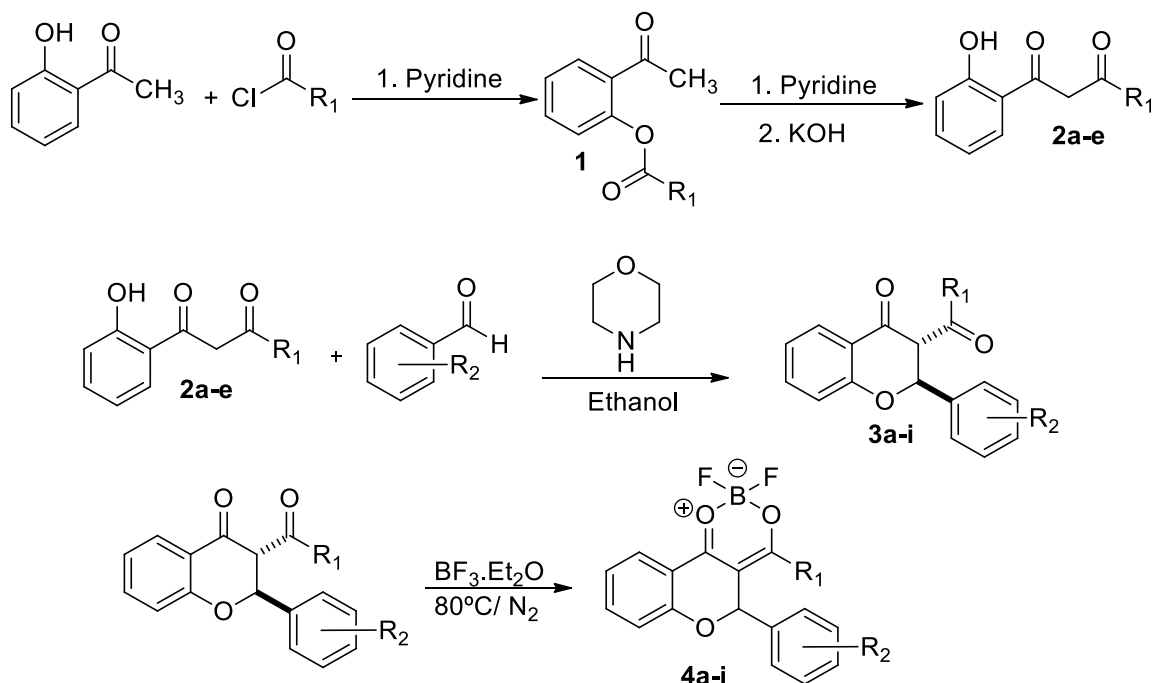
^a Chemistry Department, ICEB, Federal University of Ouro Preto, Campus Universitário Morro do Cruzeiro, 35400-000, Ouro Preto-MG, Brazil.

^b Physics Department, ICEB, Federal University of Ouro Preto, Campus Universitário Morro do Cruzeiro, 35400-000, Ouro Preto-MG, Brazil.

^cUniversity of Groningen, Zernike Institute for Advanced Materials, Nijenborgh 4, 9747 AG Groningen, The Netherlands

* e-mail address of the corresponding author: jason@iceb.ufop.br or jason@ufop.edu.br

Synthesis of Compounds 4a-i



Scheme 1. Synthesis of Difluoroboron Flavanone β -Diketonate Complexes 4a-i

The FTIR (ATR), IR spectrum calculated with B3LYP functional, ^1H NMR (400 MHz) and ^{13}C NMR (100 MHz) spectra of Compound **4a** in CDCl_3

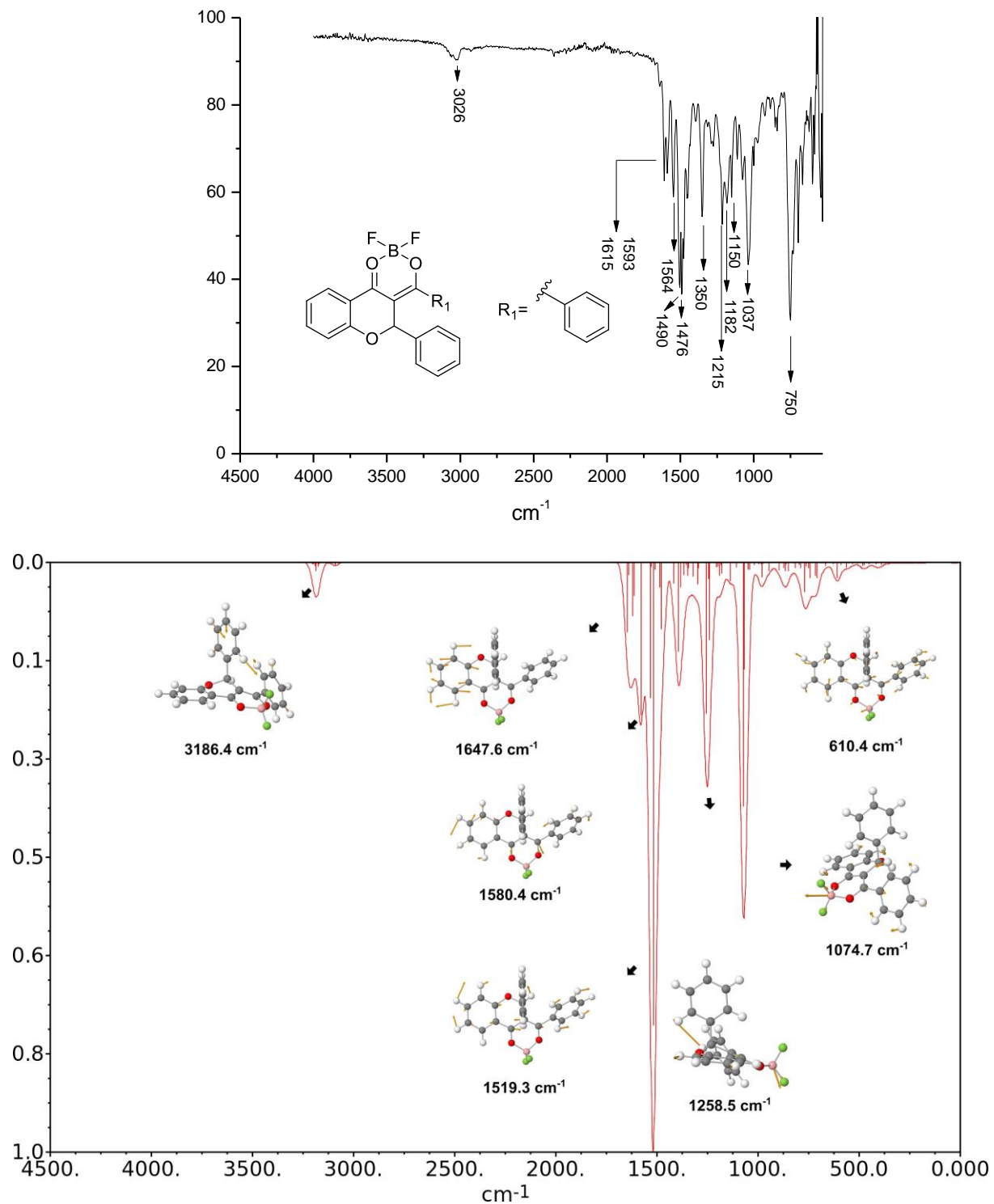


Figure 1S. Infrared spectra of compound **4a** (ATR) and IR spectrum with the main vibration normal modes for compound **4a** calculated with B3LYP functional.

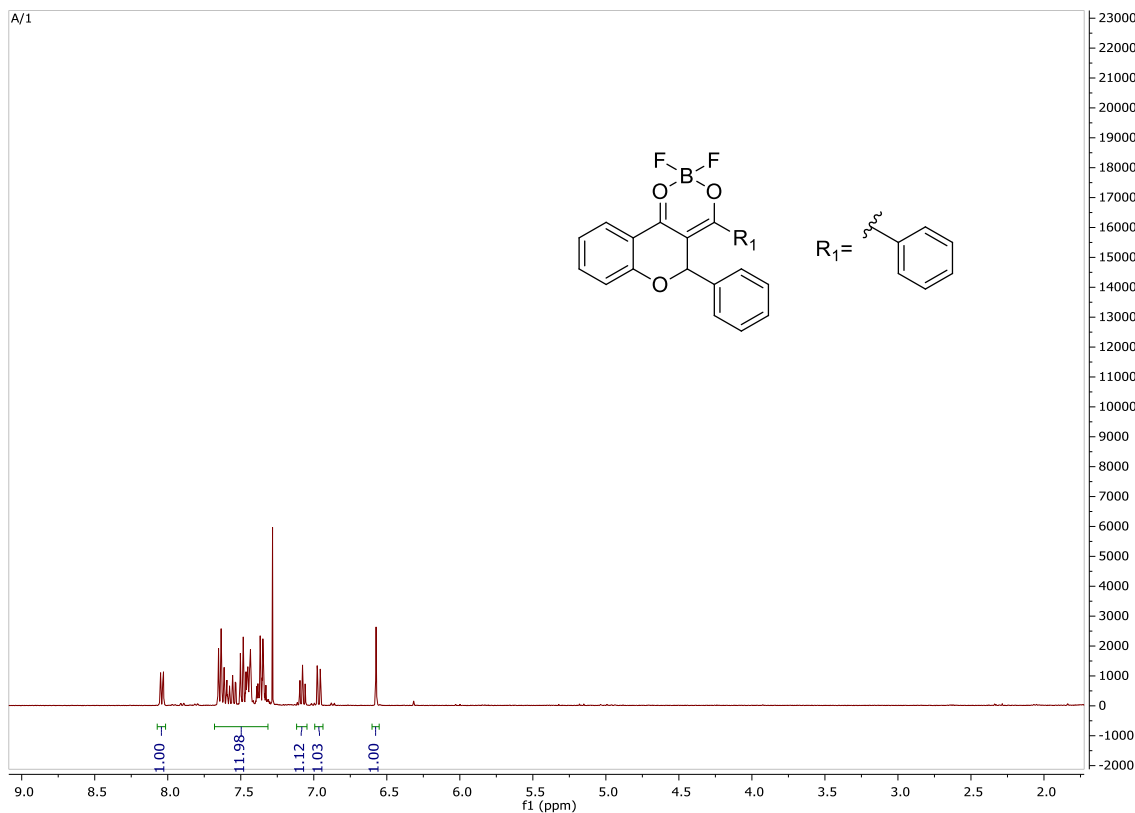


Figure 2S. NMR ^1H spectra of compound **4a** (CDCl_3 , 400 MHz)

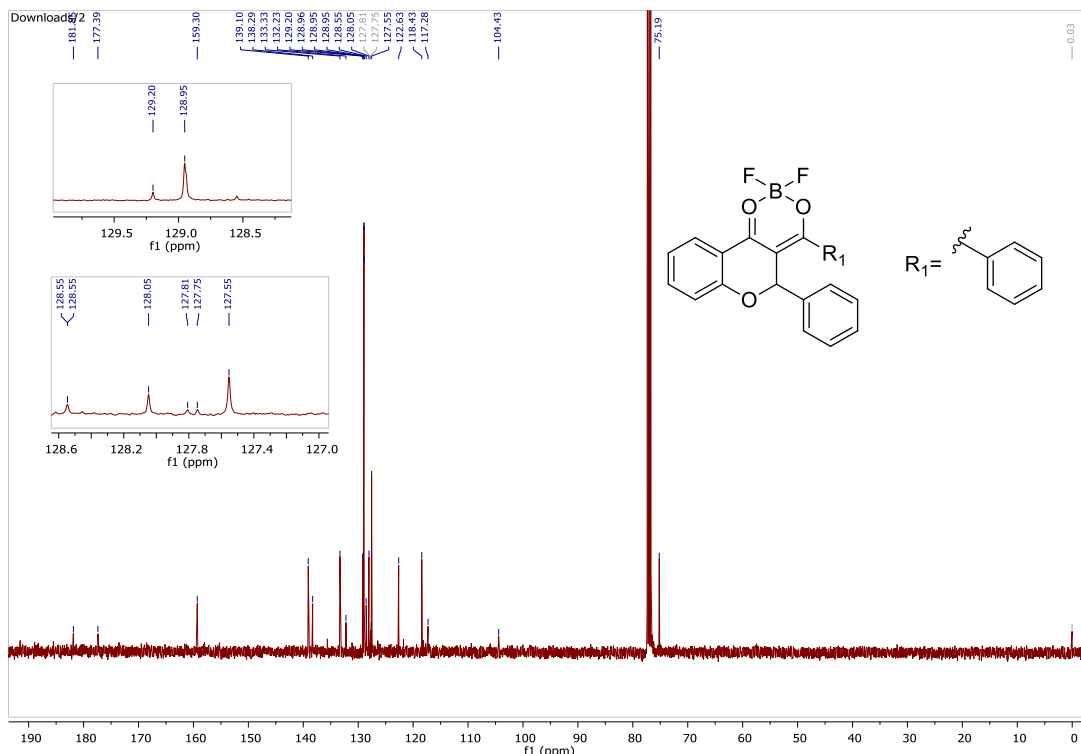


Figure 3S. NMR ^{13}C spectra of compound **4a** (CDCl_3 , 100 MHz)

The FTIR (ATR), ^1H NMR (400 MHz) and ^{13}C NMR (100 MHz) spectra of Compound **4b** in CDCl_3

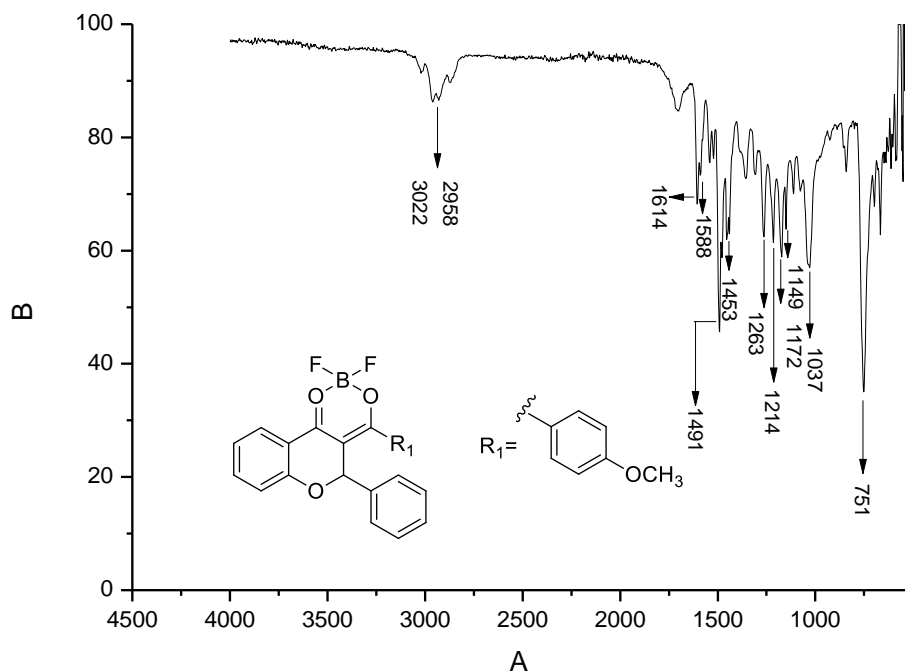


Figure 4S. Infrared spectra of compound **4b** (ATR)

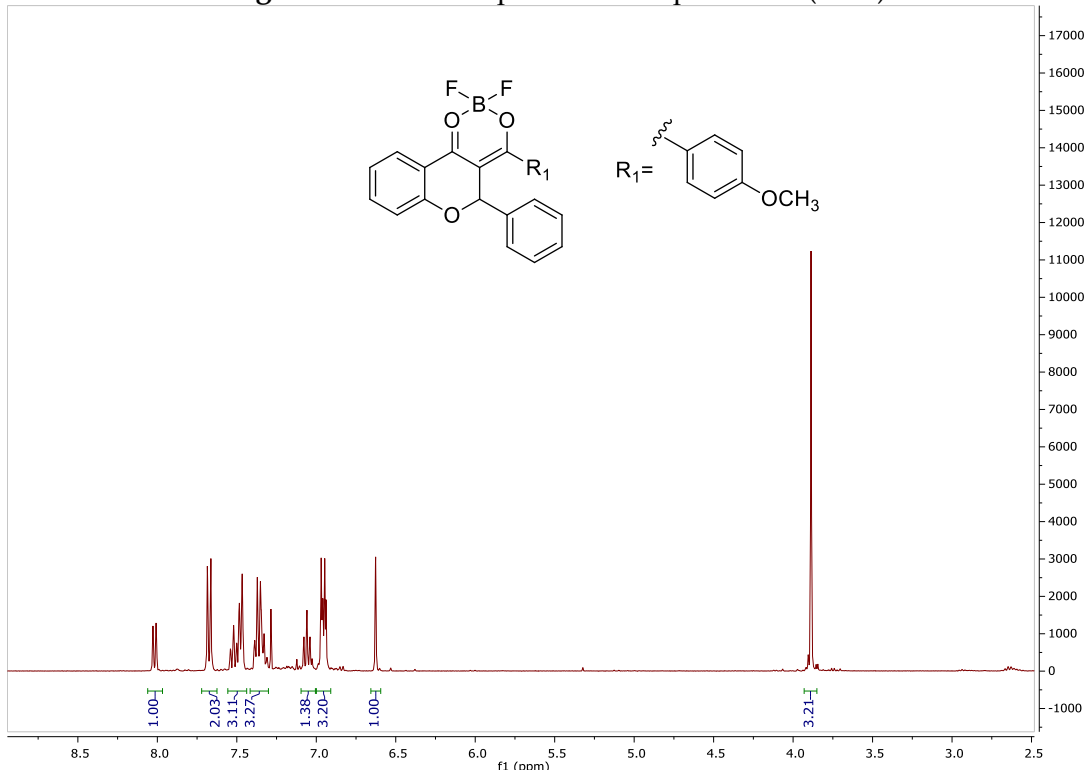


Figure 5S. NMR ^1H spectra of compound **4b** (CDCl_3 , 400 MHz)

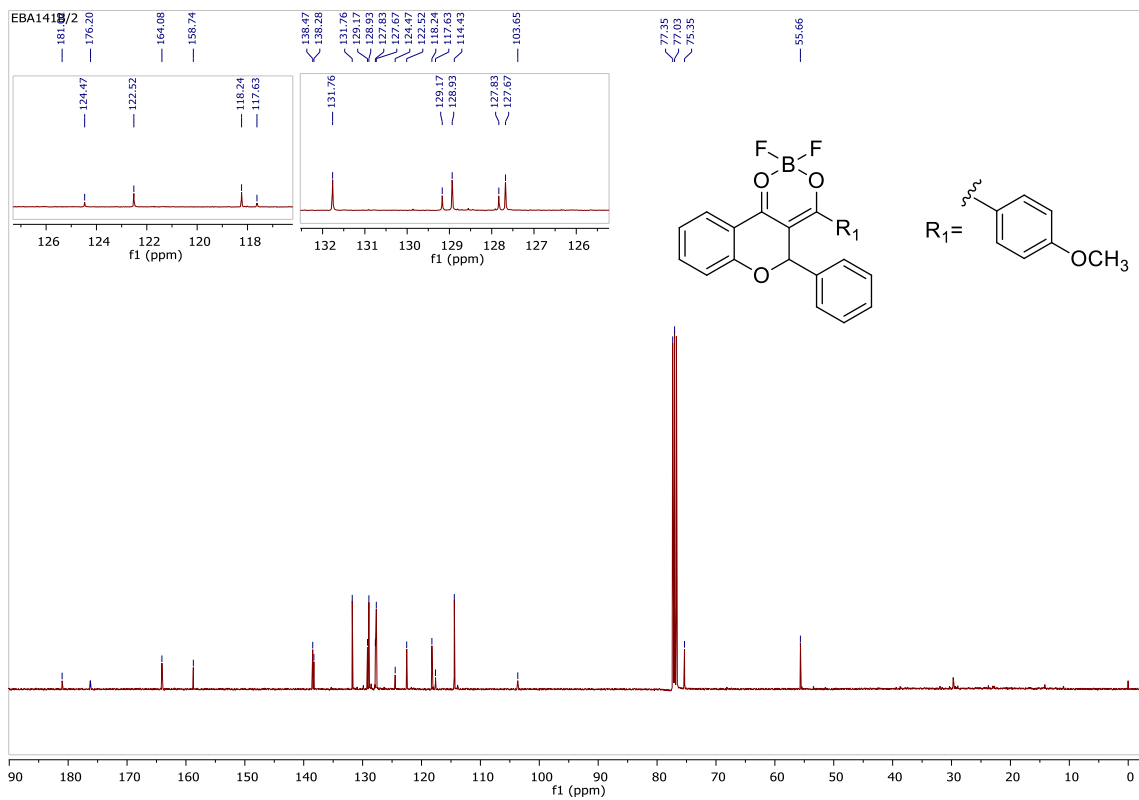


Figure 6S. NMR ¹³C spectra of compound **4b** (CDCl₃, 100 MHz)

The FTIR (ATR), ^1H NMR (400 MHz) and ^{13}C NMR (100 MHz) spectra of Compound **4c** in CDCl_3

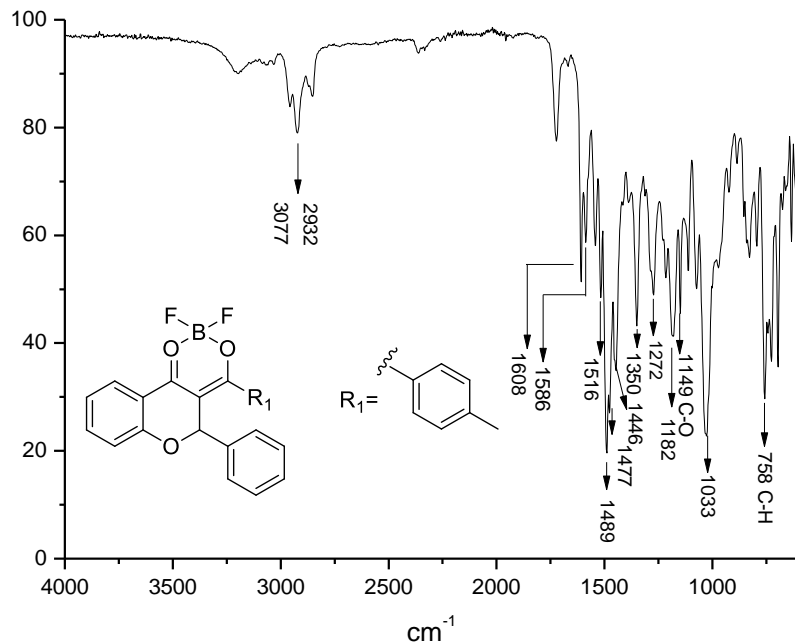


Figure 7S. Infrared spectra of compound **4c** (ATR)

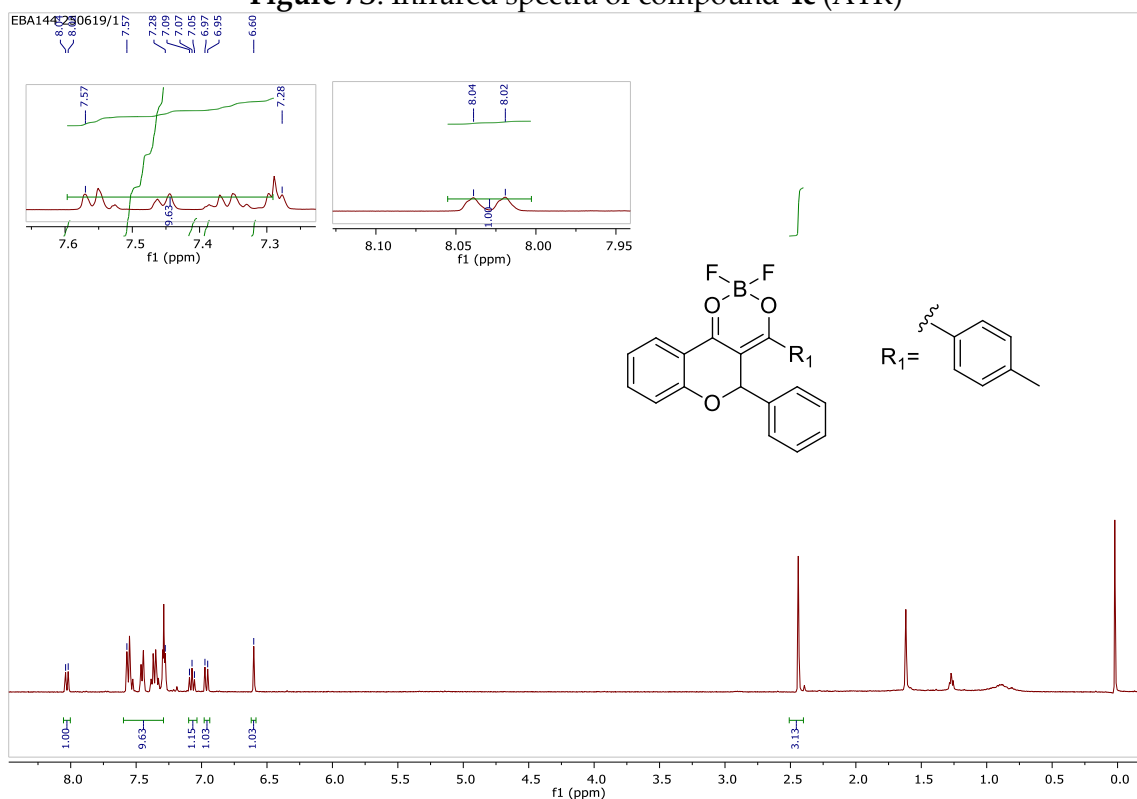


Figure 8S. NMR ^1H spectra of compound **4c** (CDCl_3 , 400 MHz)

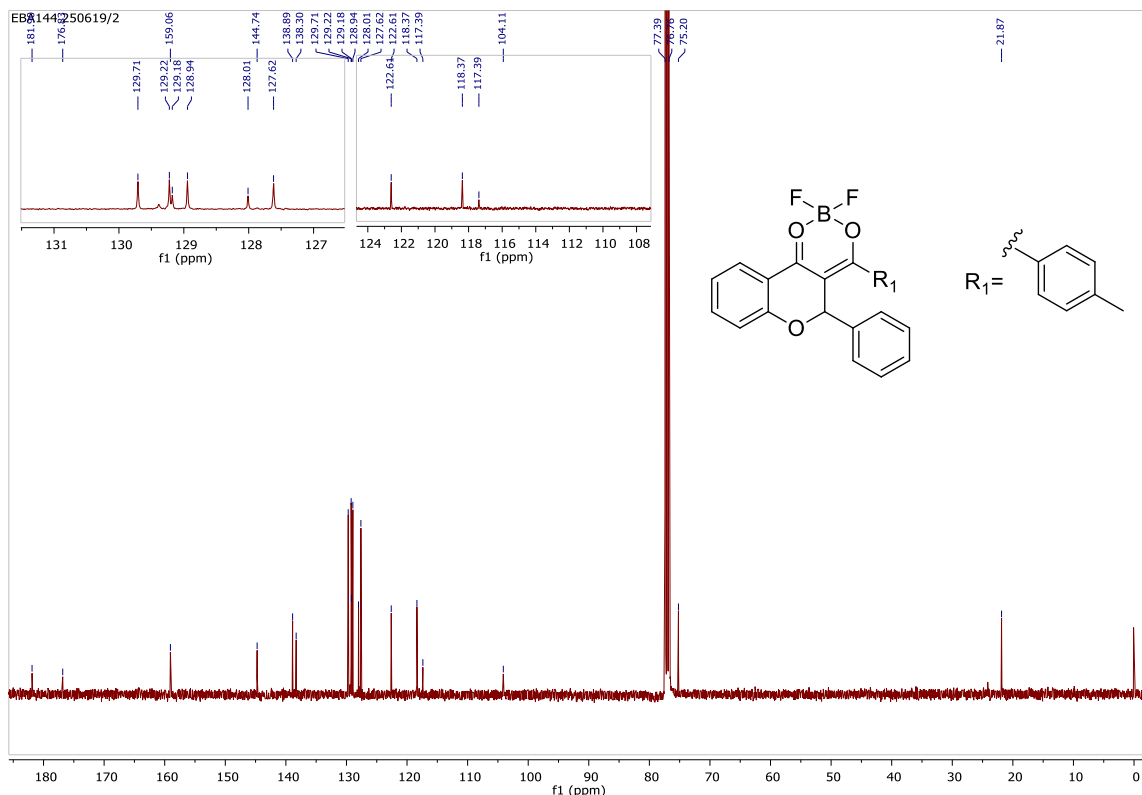


Figure 9S. NMR ¹³C spectra of compound **4c** (CDCl₃, 100 MHz)

The FTIR (ATR), ¹H NMR (400 MHz) and ¹³C NMR (100 MHz) spectra of Compound **4d** in CDCl₃

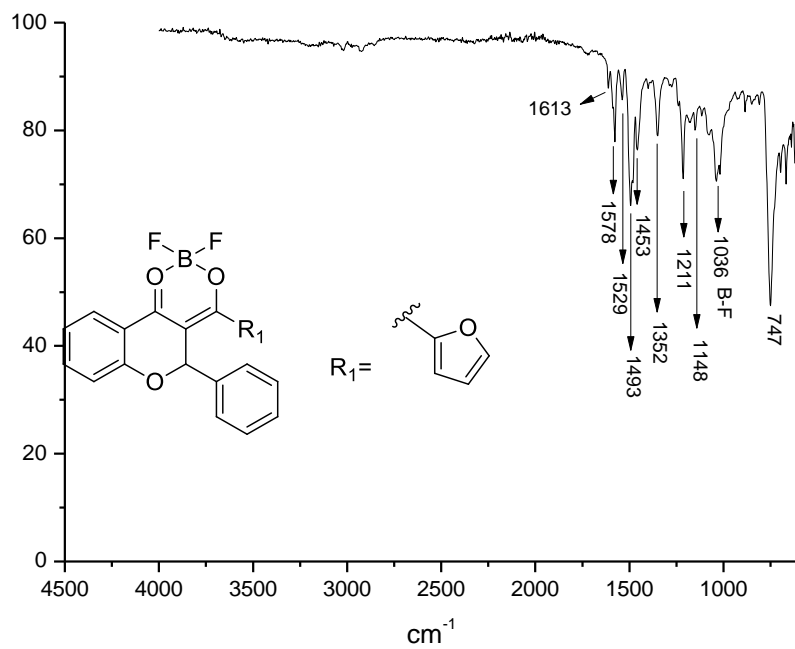


Figure 10S. Infrared spectra of compound **4d** (ATR)

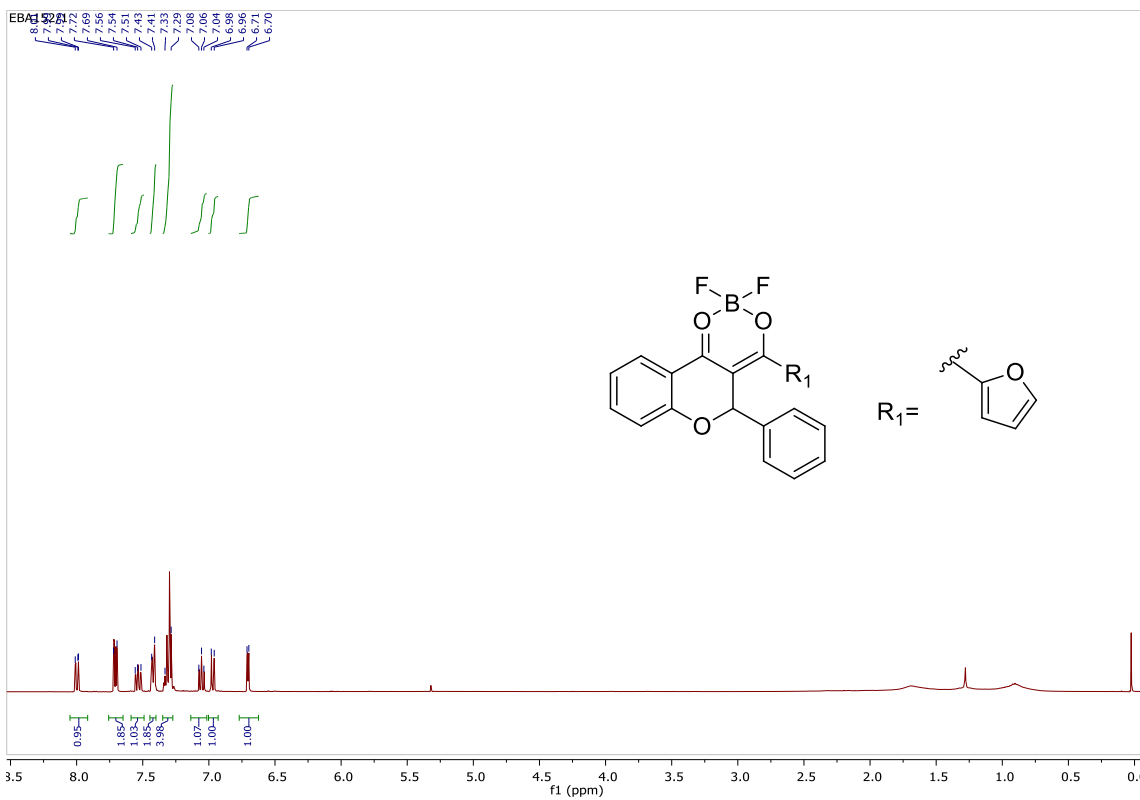


Figure 11S. NMR ^1H spectra of compound **4d** (CDCl_3 , 400 MHz)

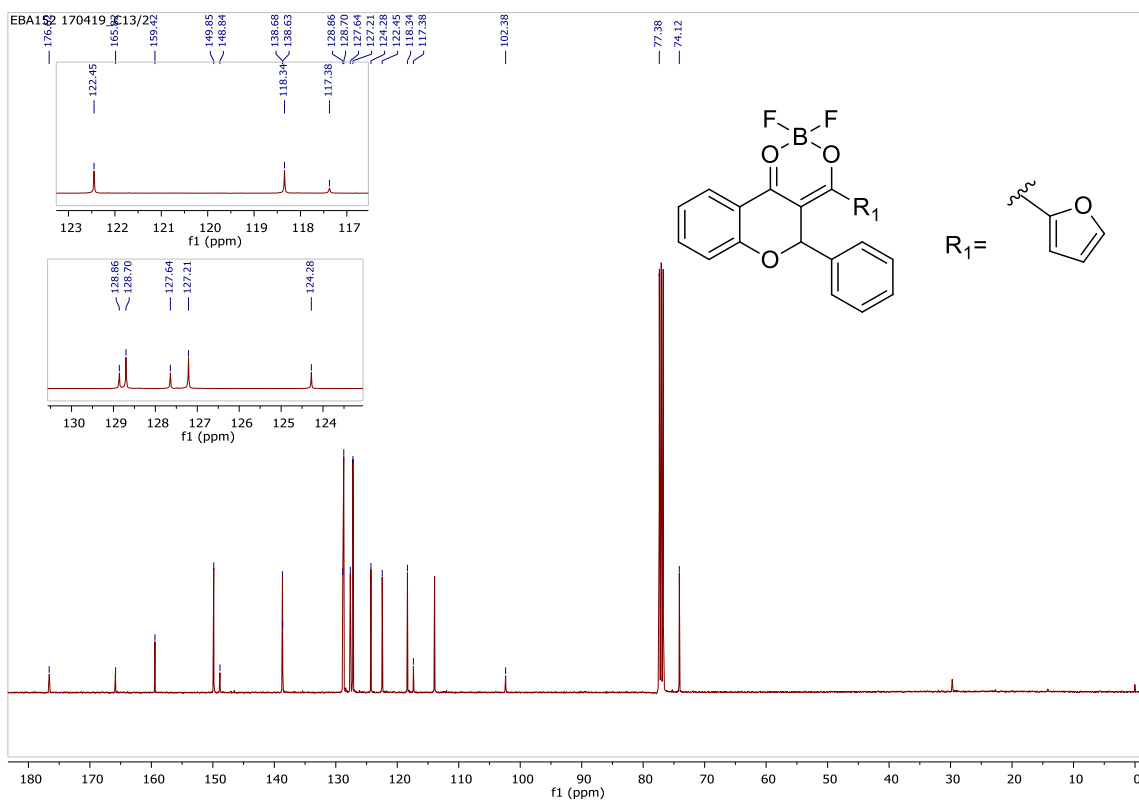


Figure 12S. NMR ^{13}C spectra of compound **4d** (CDCl_3 , 100 MHz)

The FTIR (ATR), ^1H NMR (400 MHz) and ^{13}C NMR (100 MHz) spectra of Compound **4e** in CDCl_3

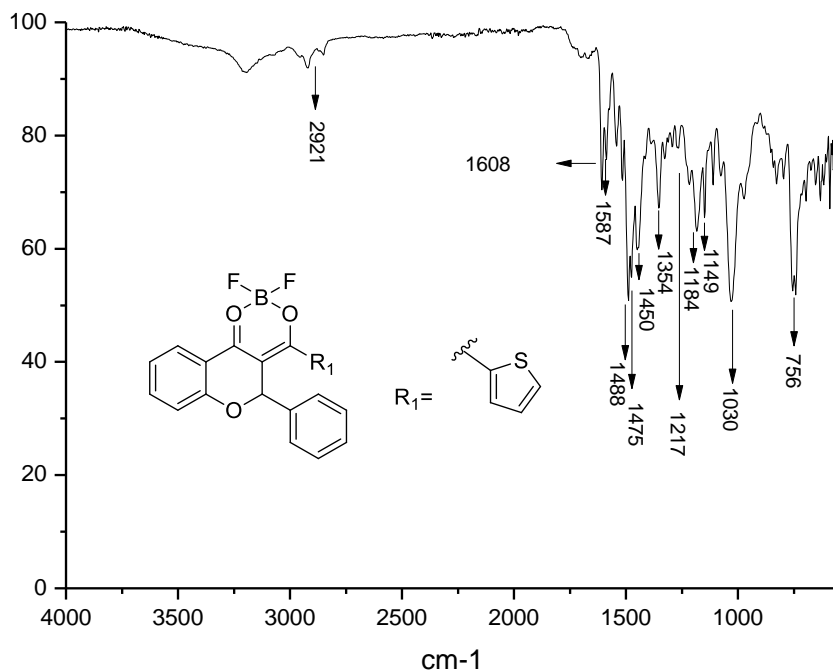


Figure 13S. Infrared spectra of compound **4e** (ATR)

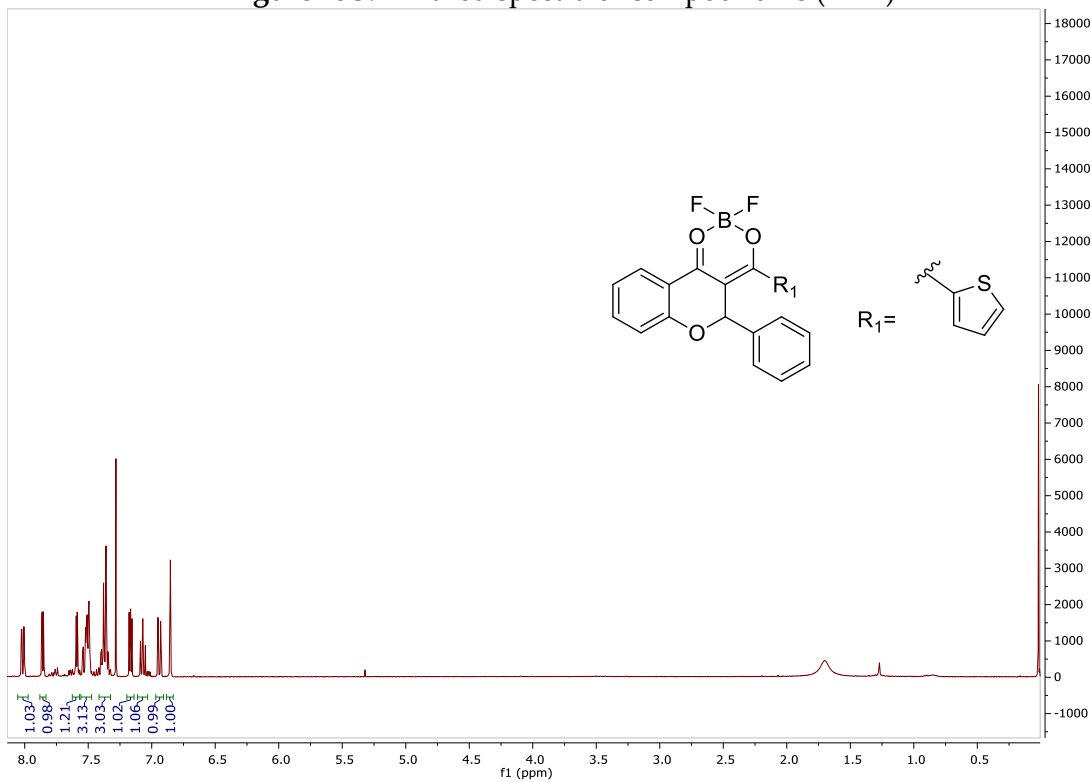


Figure 14S. NMR ^1H spectra of compound **4e** (CDCl_3 , 400 MHz)

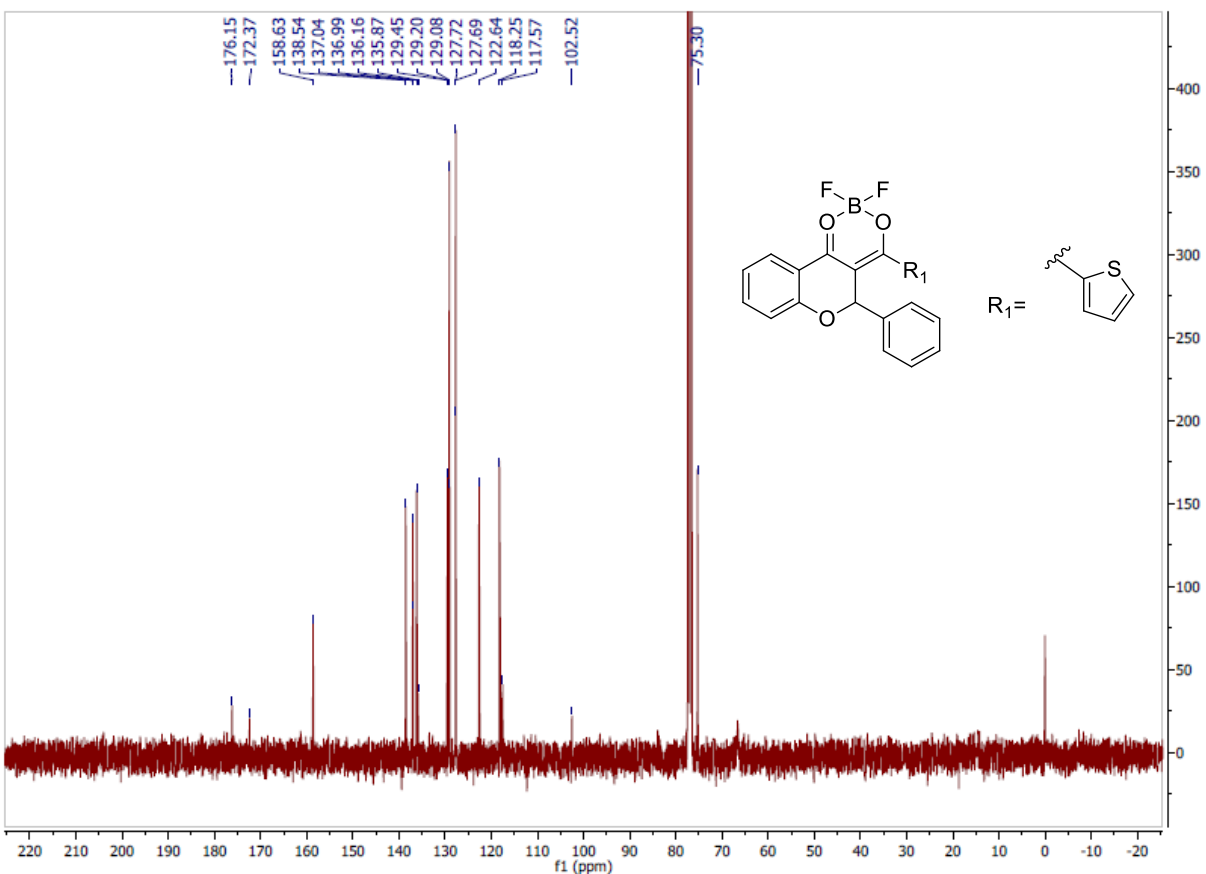


Figure 15S. NMR ^{13}C spectra of compound **4e** (CDCl_3 , 100 MHz)

The FTIR (ATR), ^1H NMR (400 MHz) and ^{13}C NMR (100 MHz) spectra of Compound **4f** in CDCl_3

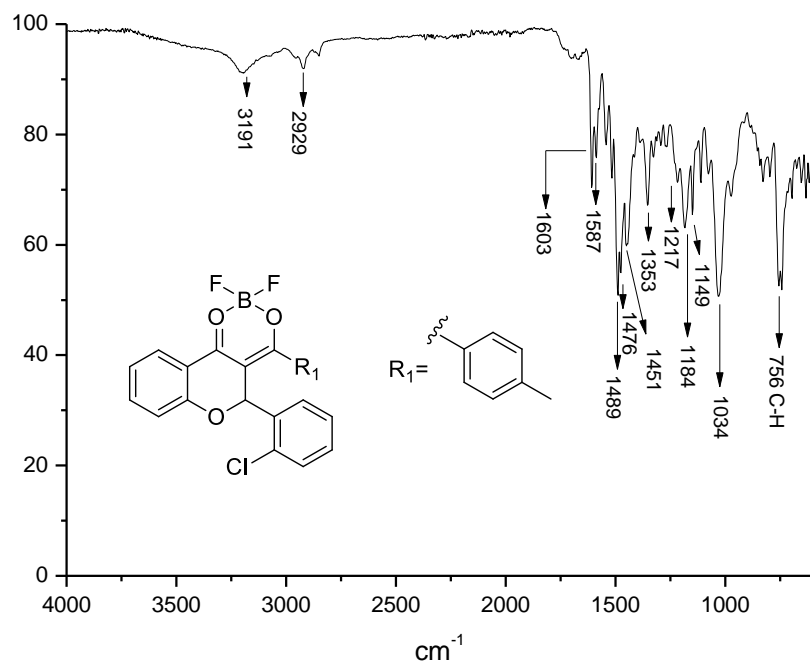


Figure 16S. Infrared spectra of compound **4f** (ATR)

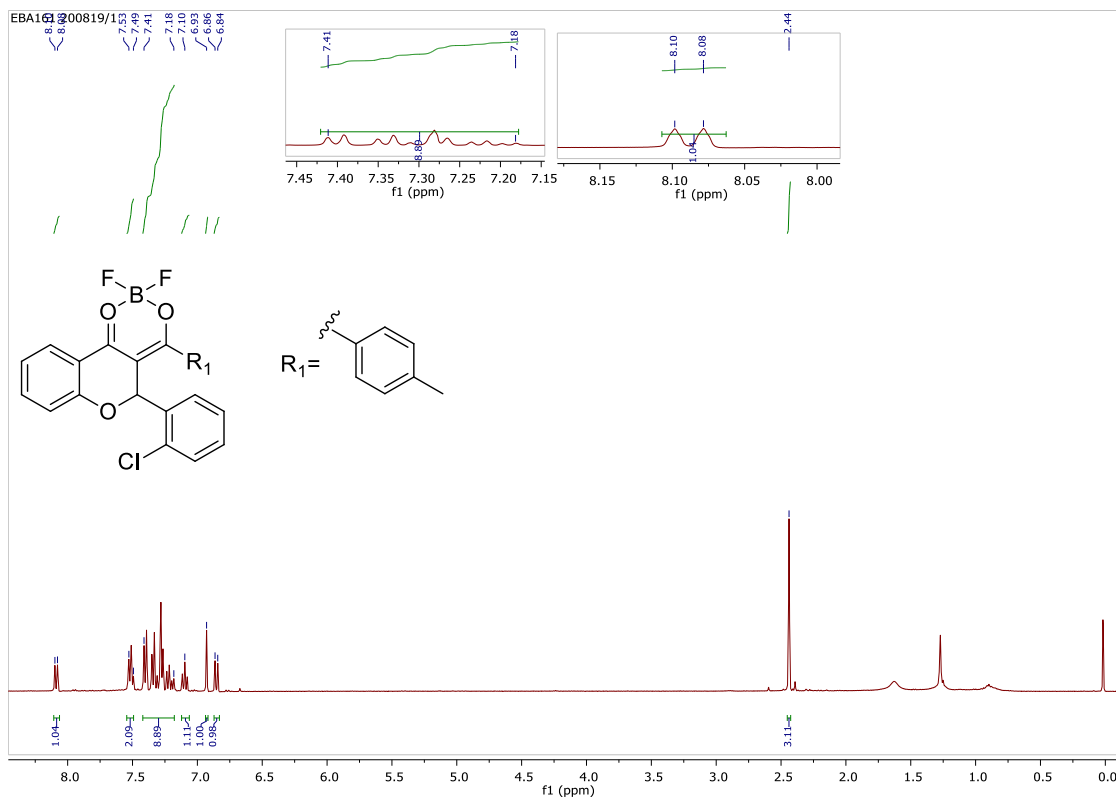


Figure 17S. NMR ^1H spectra of compound **4f** (CDCl_3 , 400 MHz)

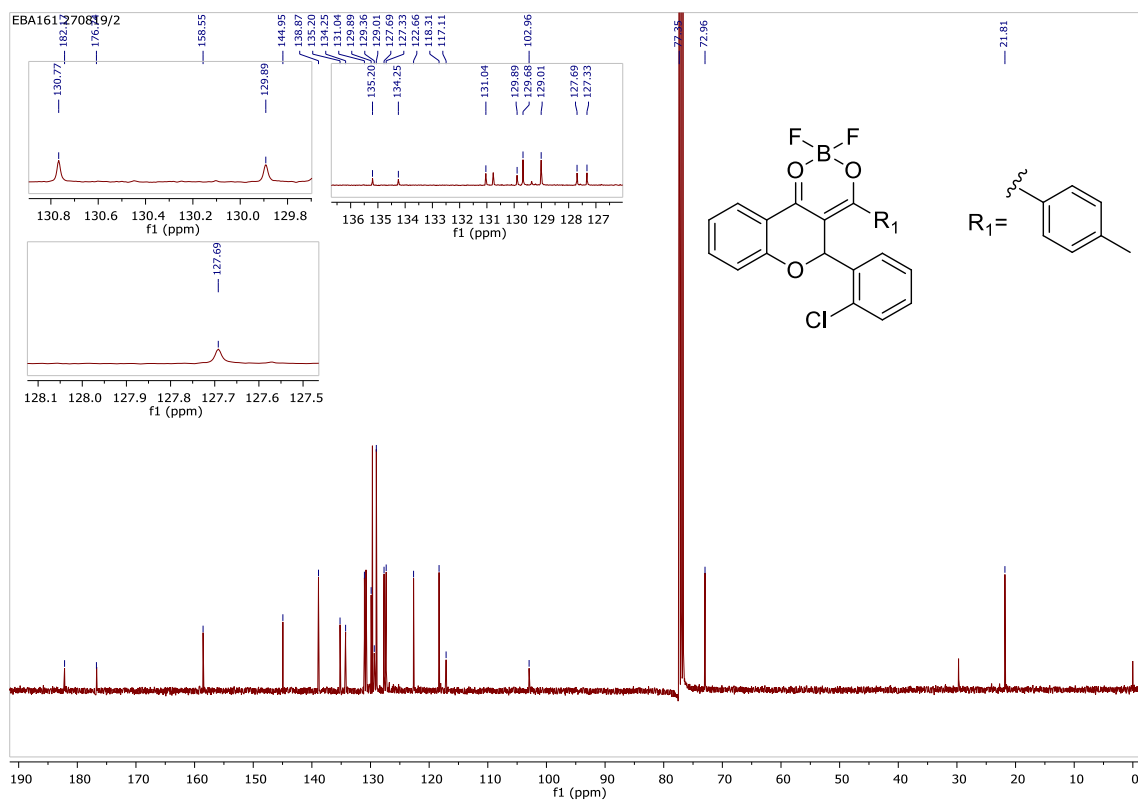


Figure 18S. NMR ^{13}C spectra of compound **4f** (CDCl_3 , 100 MHz)

The FTIR (ATR), ^1H NMR (400 MHz) and ^{13}C NMR (100 MHz) spectra of Compound **4g** in CDCl_3

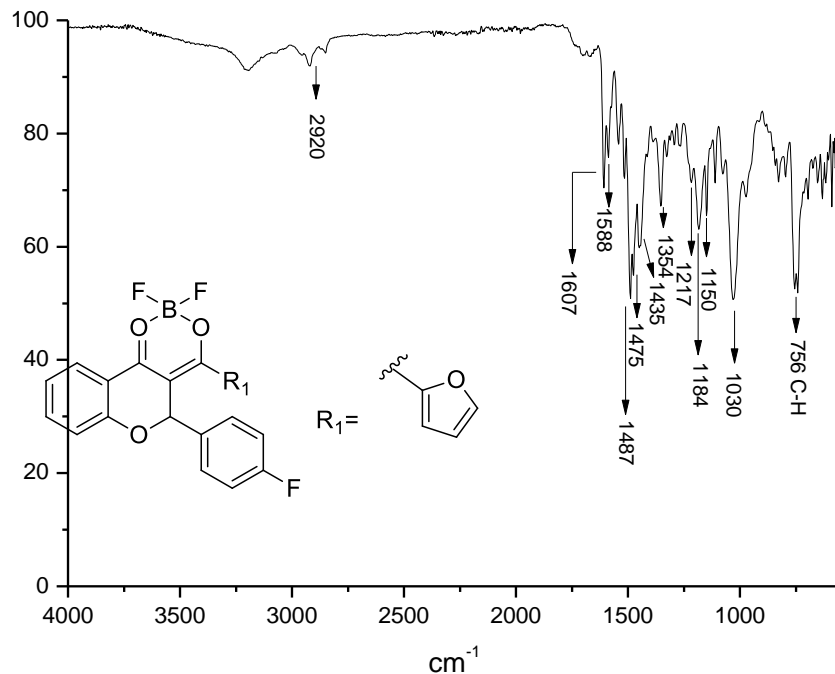


Figure 19S. Infrared spectra of compound **4g** (ATR)

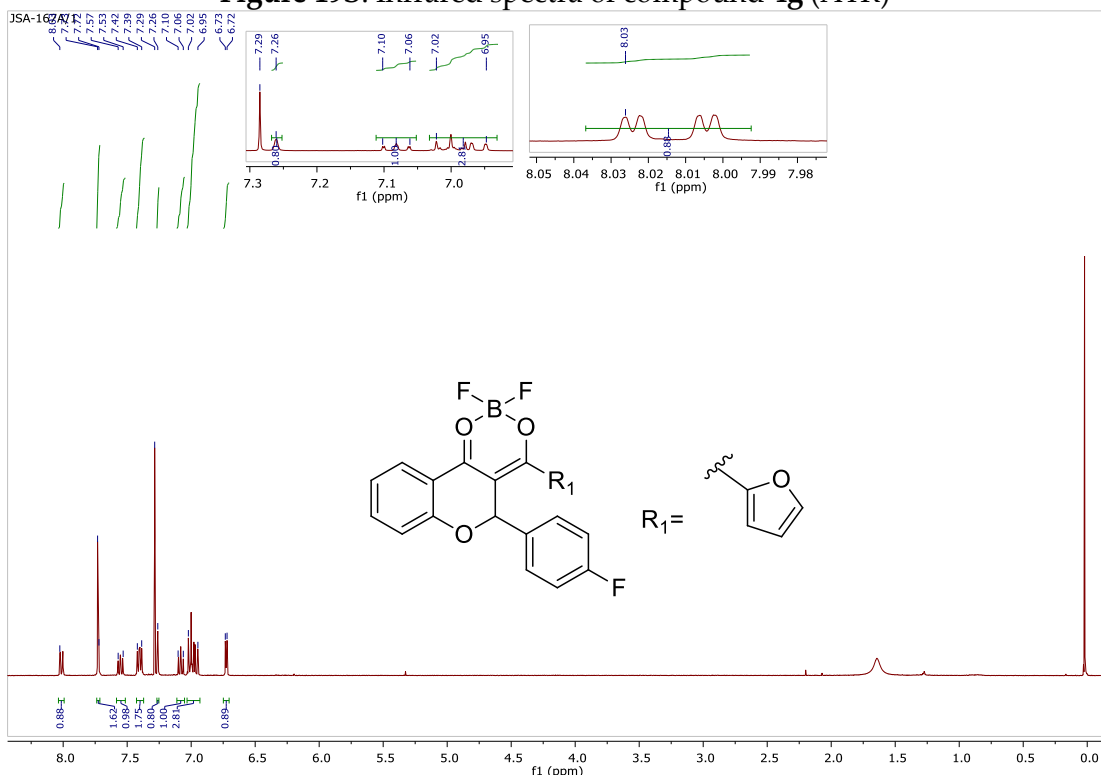


Figure 20S. NMR ^1H spectra of compound **4g** (CDCl_3 , 400 MHz)

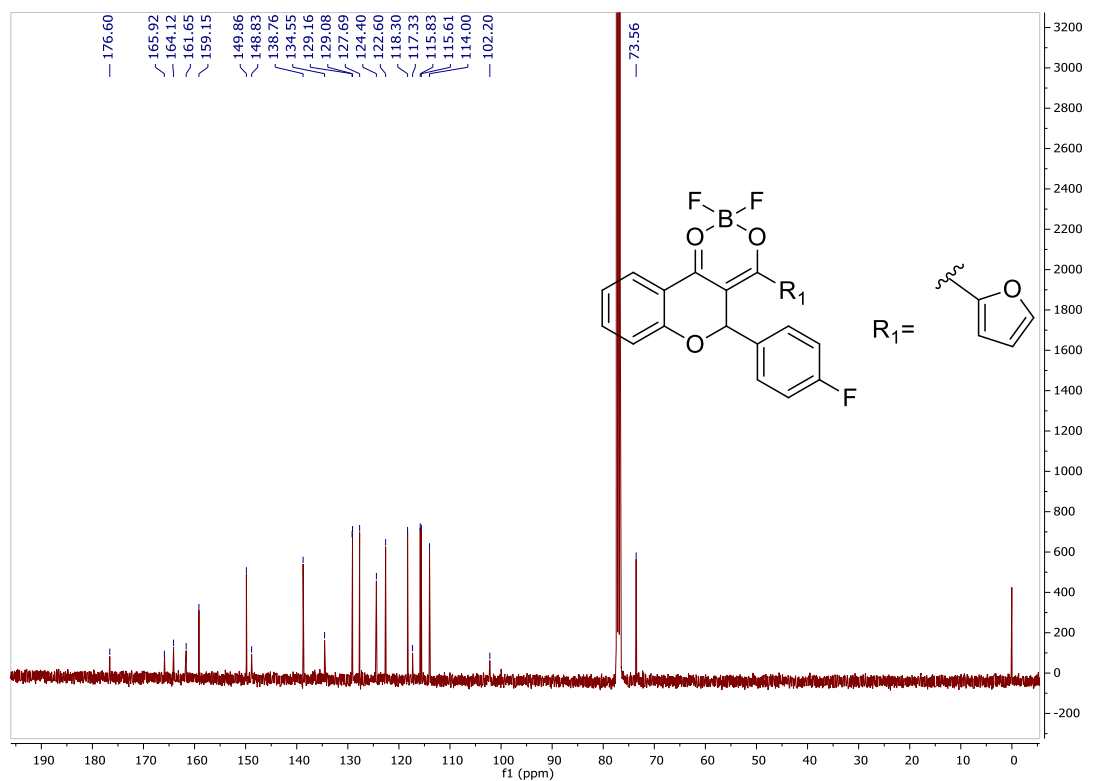


Figure 21S. NMR ^{13}C spectra of compound **4g** (CDCl_3 , 100 MHz)

The FTIR (ATR), ^1H NMR (400 MHz) and ^{13}C NMR (100 MHz) spectra of Compound **4h** in CDCl_3

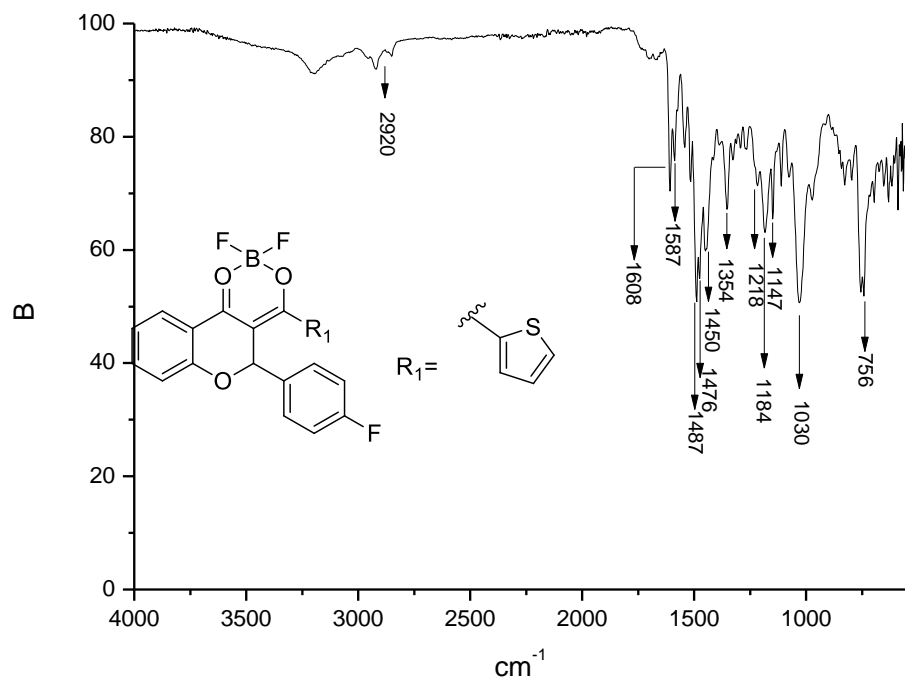


Figure 22S. Infrared spectra of compound **4h** (ATR)

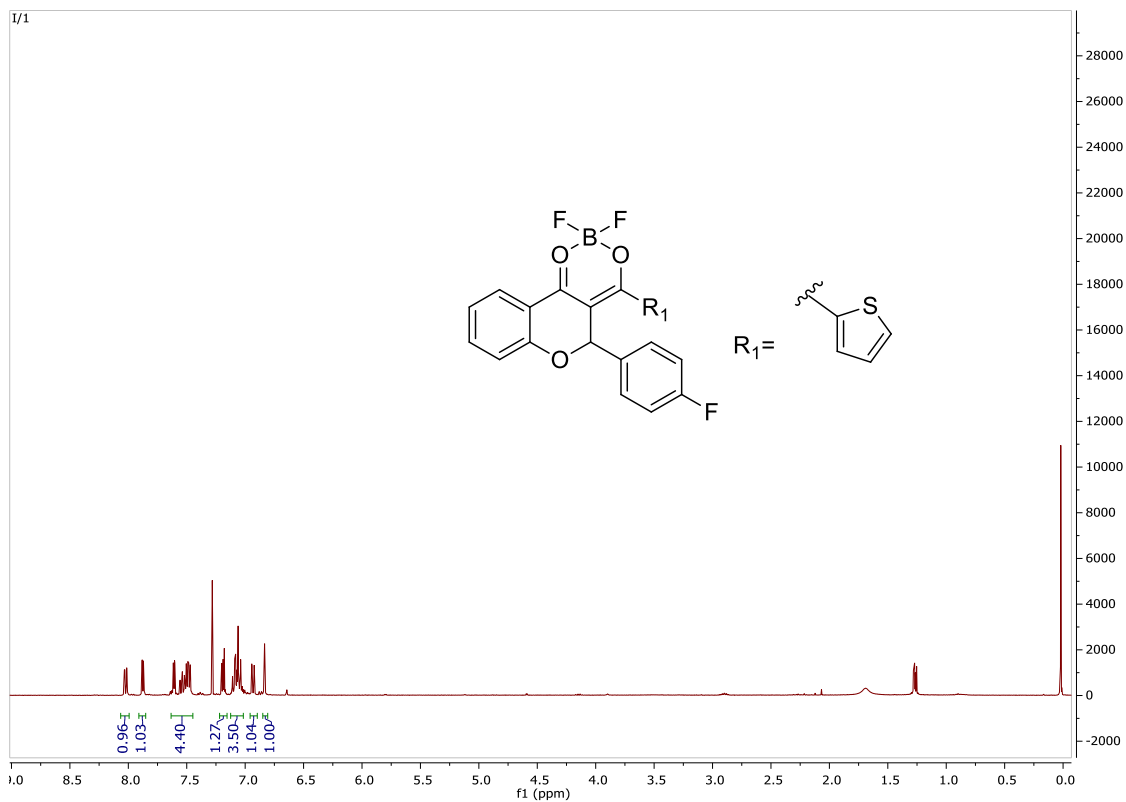


Figure 23S. NMR ¹H spectra of compound **4h** (CDCl₃, 400 MHz)

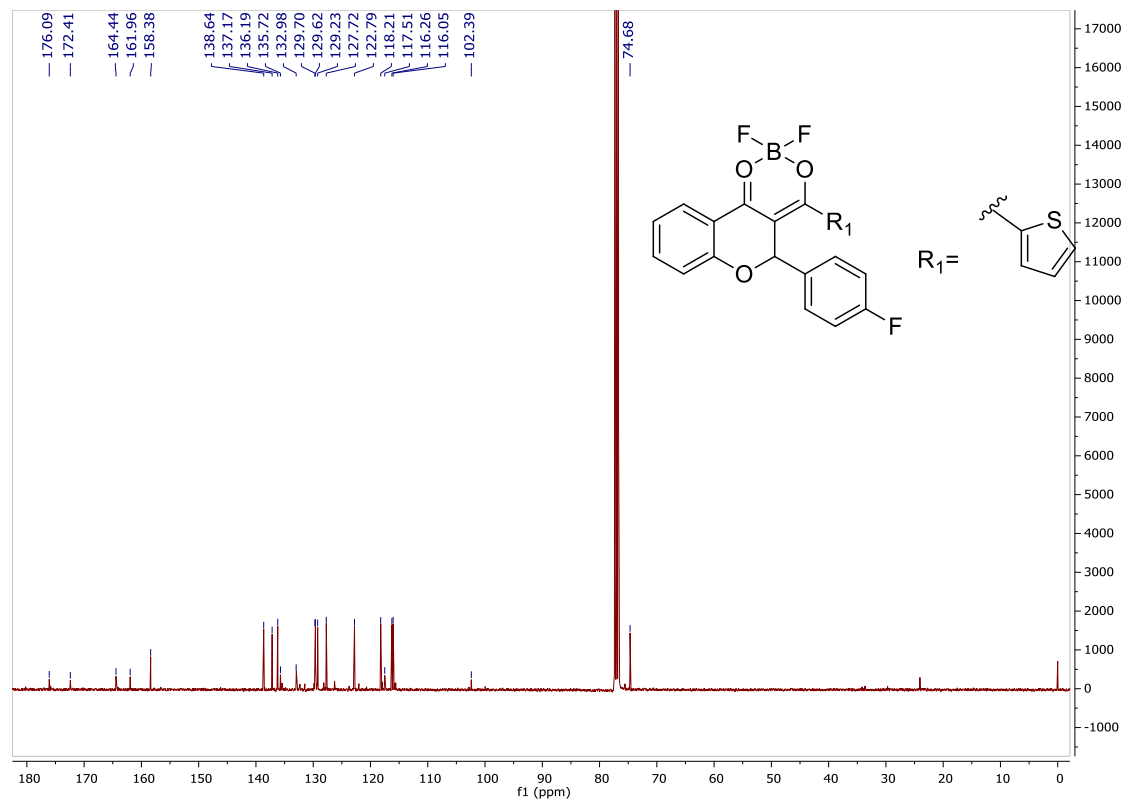


Figure 24S. NMR ¹³C spectra of compound **4h** (CDCl₃, 100 MHz)

The FTIR (ATR), ^1H NMR (400 MHz) and ^{13}C NMR (100 MHz) spectra of Compound **4i** in CDCl_3

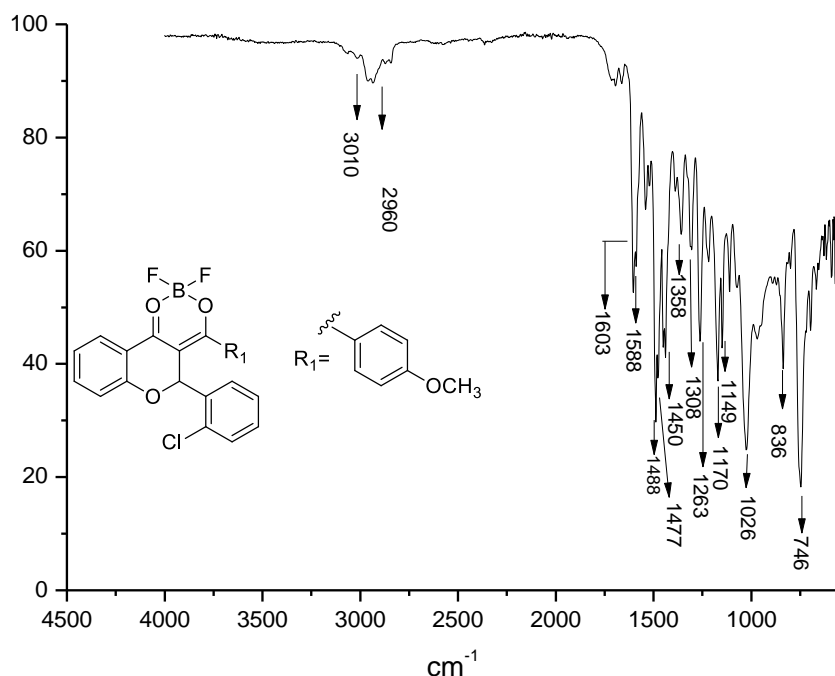


Figure 25S. Infrared spectra of compound **4i** (ATR)

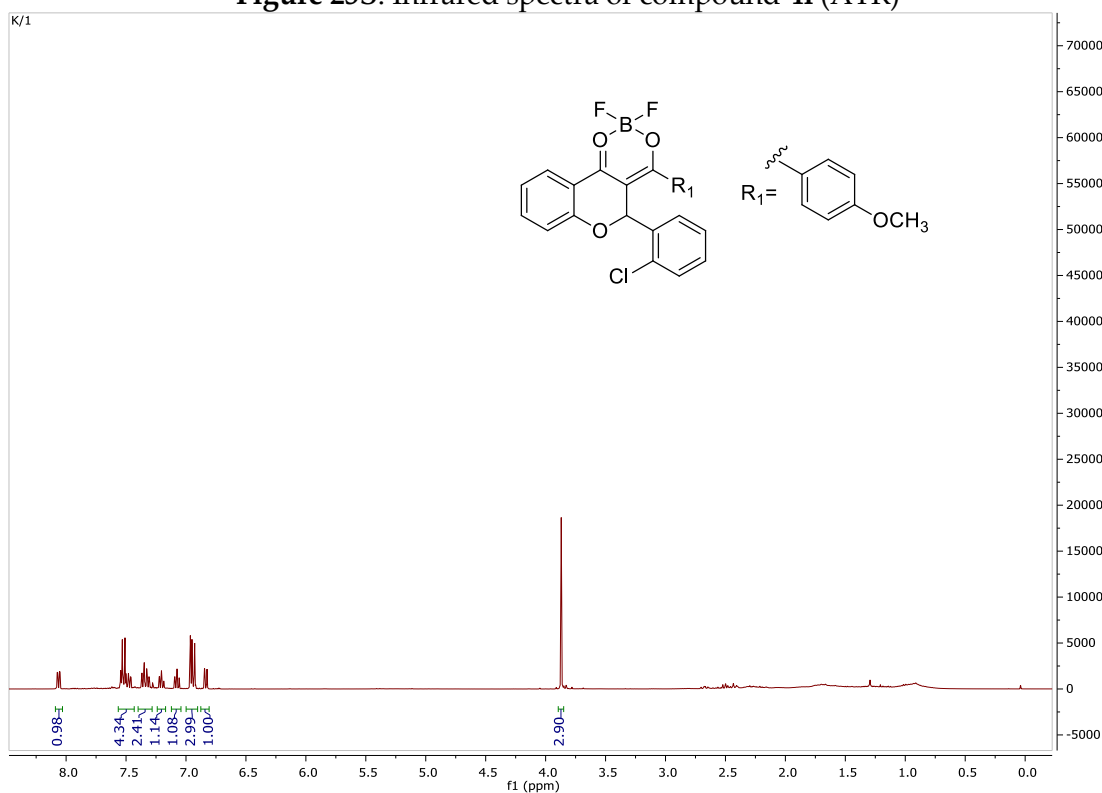


Figure 26S. NMR ^1H spectra of compound **4i** (CDCl_3 , 400 MHz)

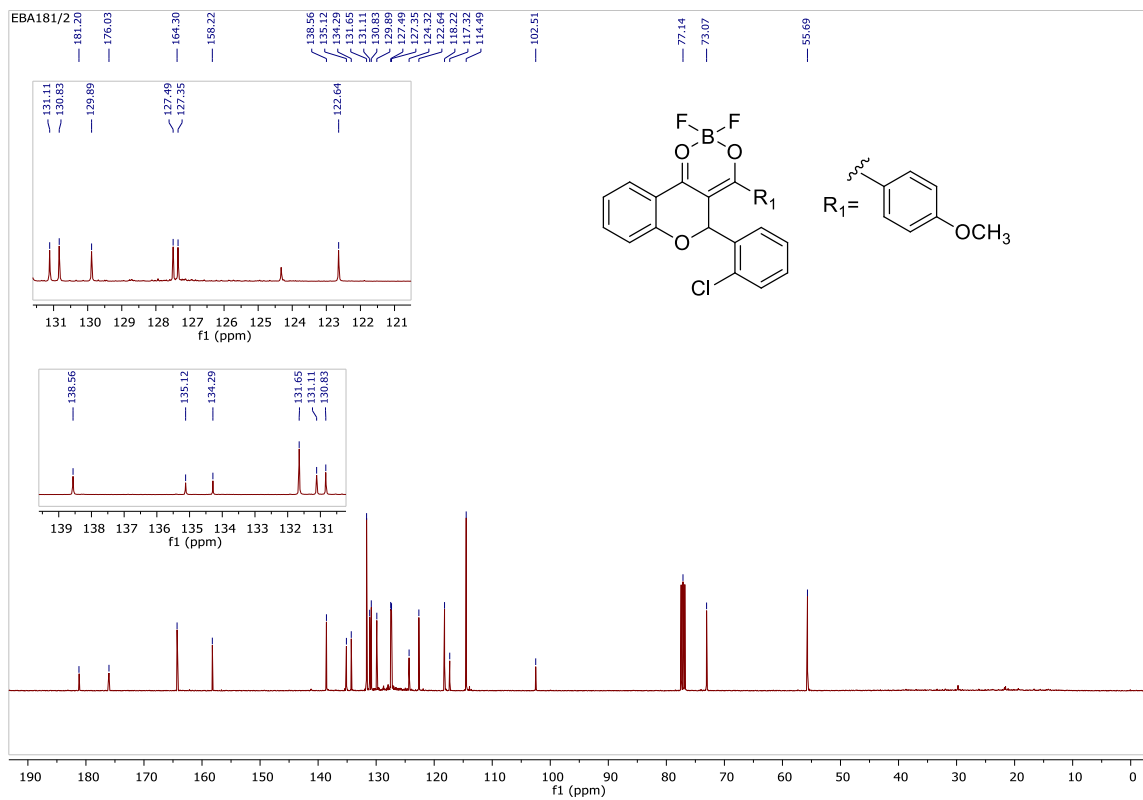


Figure 27S. NMR ^{13}C spectra of compound **4i** (CDCl_3 , 400 MHz)

Crystallographic Data and Refinement for compound 4e

Table 1S. Crystallographic data and refinement structure of compound 4e

Empirical formula	C ₂₀ H ₁₃ BF ₂ O ₃ S
Formula weight	382.17
Temperature	298(2) K
Wavelength	1.54184 Å
Crystal system	Monoclinic
Space group	P2 ₁ /c
Unit cell dimensions	a = 10.1117(5) Å b = 18.9112(6) Å; β = 117.599(6)°. c = 10.1323(5) Å V = 1717.07(16) Å ³
Volume	1717.07(16) Å ³
Z	4
Density (calculated)	1.478 Mg/m ³
Absorption coefficient	2.033 mm ⁻¹
F(000)	784
Crystal size	0.23 x 0.11 x 0.10 mm ³
Theta range for data collection	4.677 to 87.018°.
Index ranges	-12≤h≤13, -23≤k≤22, -13≤l≤12
Reflections collected	22177
Independent reflections	3526 [R(int) = 0.1595]
Completeness to theta = 67.684°	99.9 %
Data / restraints / parameters	3526 / 0 / 302
Goodness-of-fit on F ²	1.095
Final R indices [I>2sigma(I)]	R1 = 0.0689, wR2 = 0.1871
R indices (all data)	R1 = 0.0868, wR2 = 0.2190
Extinction coefficient	0.0017(4)
Largest diff. peak and hole	0.250 and -0.329 e.Å ⁻³

Table 2S. Selected lengths (Å) and connection angles (°) for compound 4e

Bond	Length (Å)	Bond	Angle (°)
O(2)-C(3)	1.307(3)	C(3)-O(2)-B(1)	120.6(3)
O(1)-C(1)	1.316(3)	C(1)-O(1)-B(1)	122.2(2)
O(2)-B(1)	1.476(5)	F(1)-B(1)-F(2)	112.1(3)
O(1)-B(1)	1.458(5)	F(1)-B(1)-O(1)	109.0(3)
F(2)-B(1)	1.371(5)	F(2)-B(1)-O(1)	108.3(4)
F(1)-B(1)	1.361(4)	F(1)-B(1)-O(2)	108.4(4)
C(3)-C(2)	1.380(4)	F(2)-B(1)-O(2)	109.4(3)
C(3)-C(4)	1.439(4)	O(1)-B(1)-O(2)	109.7(2)
C(2)-C(1)	1.402(4)	O(2)-C(3)-C(2)	122.1(3)
C(2)-C(14)	1.513(3)	O(2)-C(3)-C(4)	115.3(3)
C(14)-C(15)	1.518(3)	C(2)-C(3)-C(4)	122.6(2)
C(10)-S(1)	1.598(10)	C(3)-C(2)-C(1)	118.4(2)
C(10)-C(11)	1.635(12)	C(3)-C(2)-C(14)	119.4(2)
C(12)-C(11)	1.572(16)	C(10)-S(1)-C(13)	95.5(8)
C(4)-C(9)	1.317(8)	C(4)-C(9)-O(3)	129.0(6)

C(4)-C(5) | 1.418(4) | C(4)-C(9)-C(8) | 115.4(7)

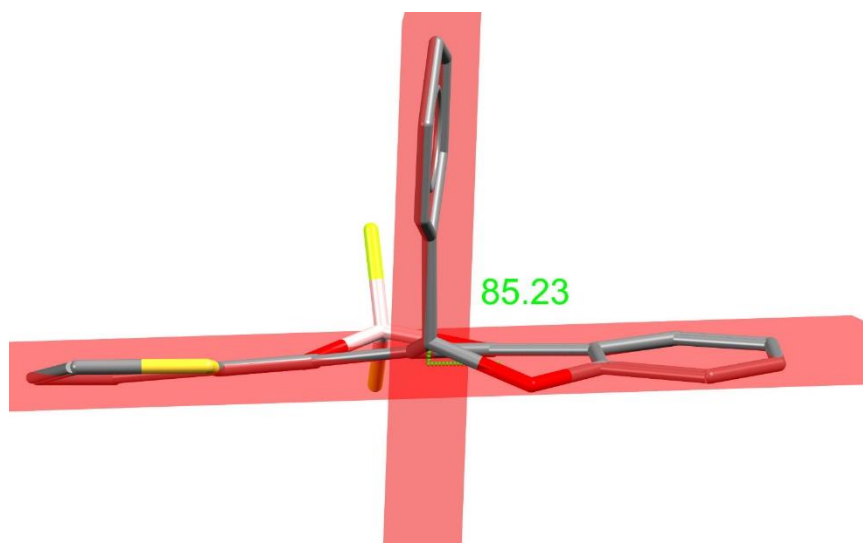
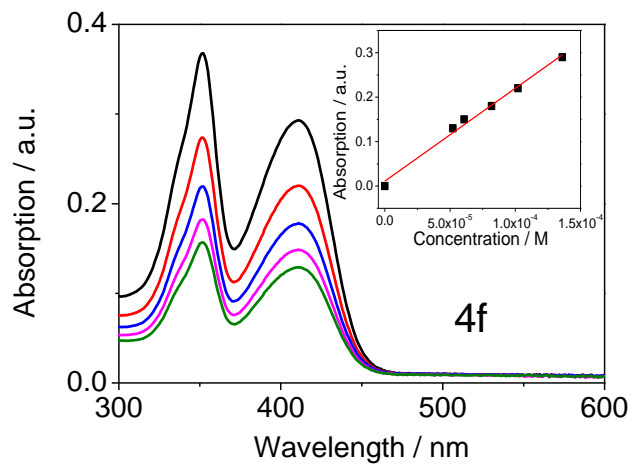
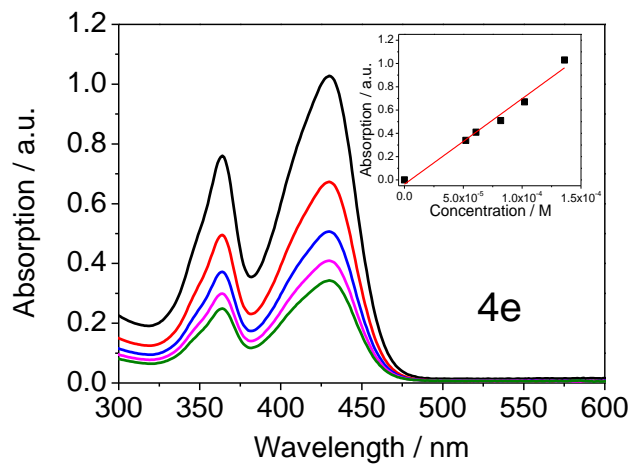
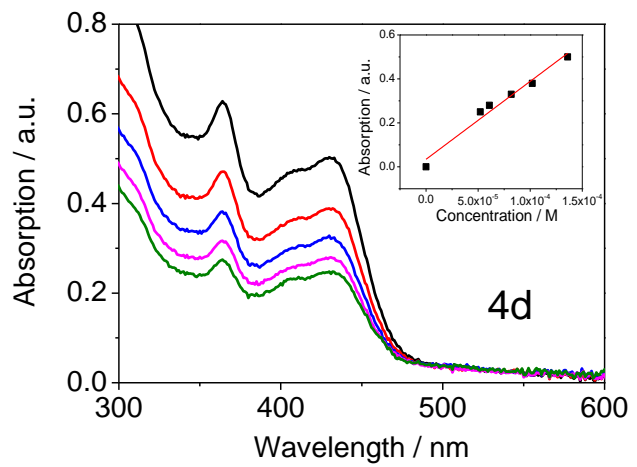
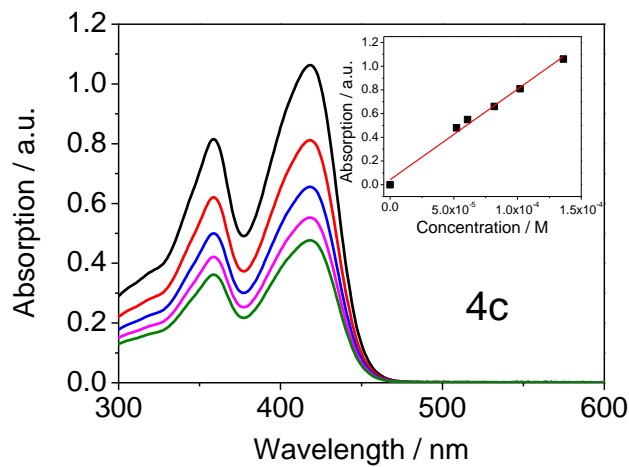
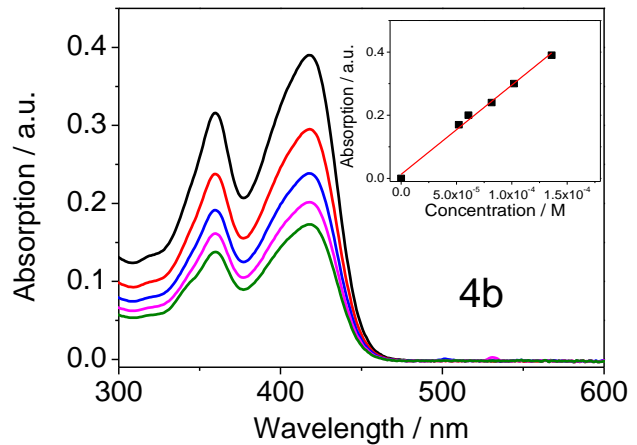
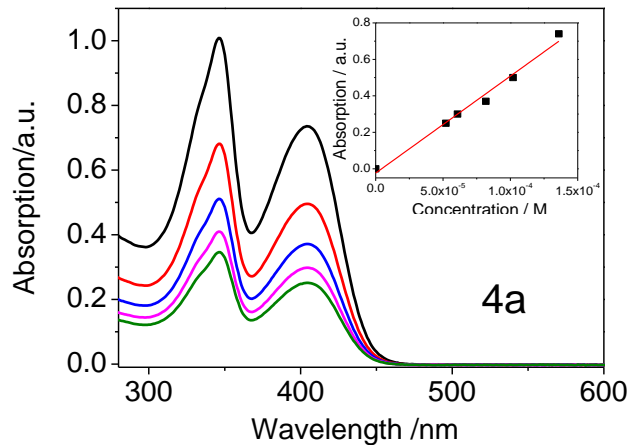


Figure 28S. X-ray structure showing molecule **4e** conformation.

Absorption spectra of the compounds with concentration vs absorption plots



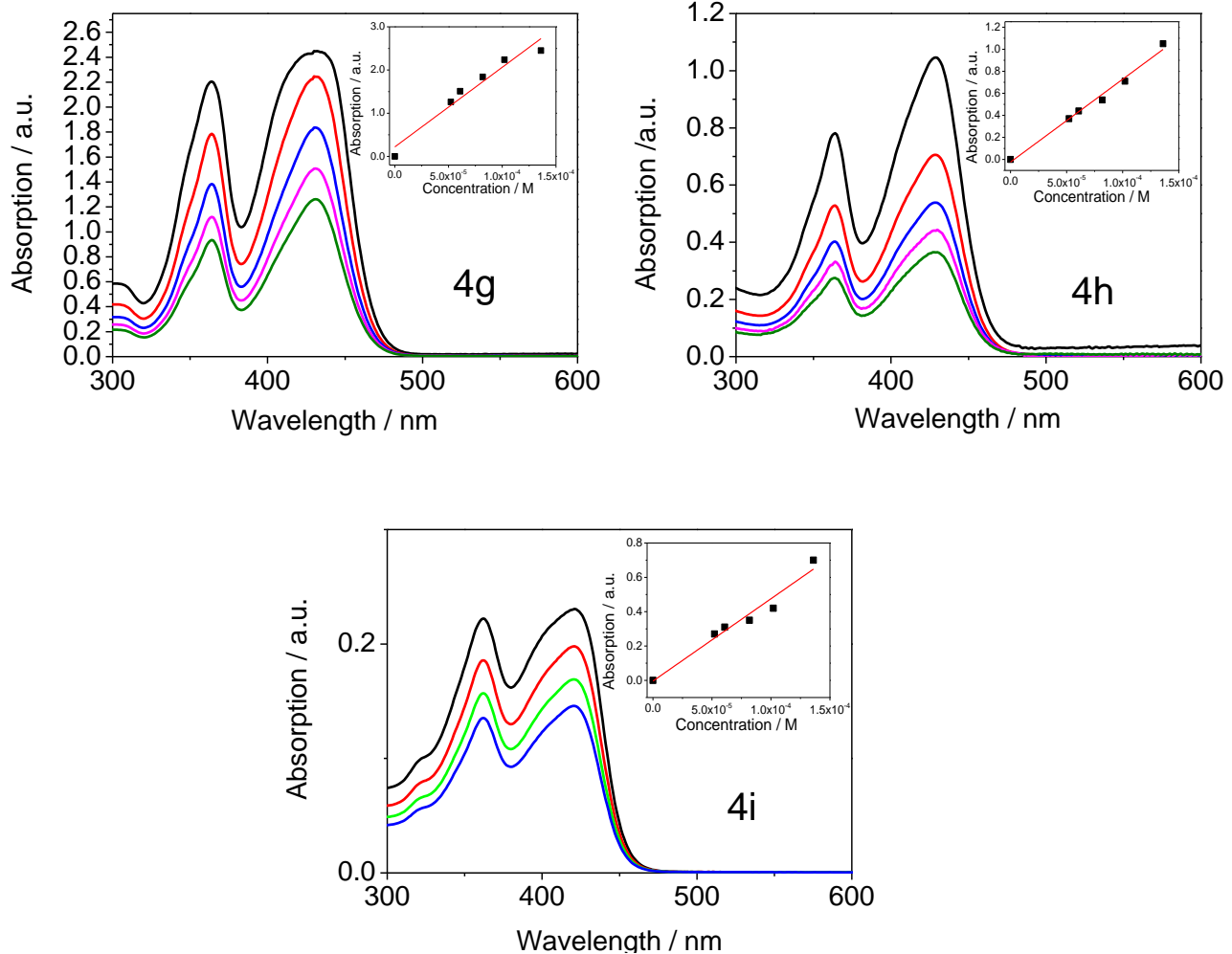
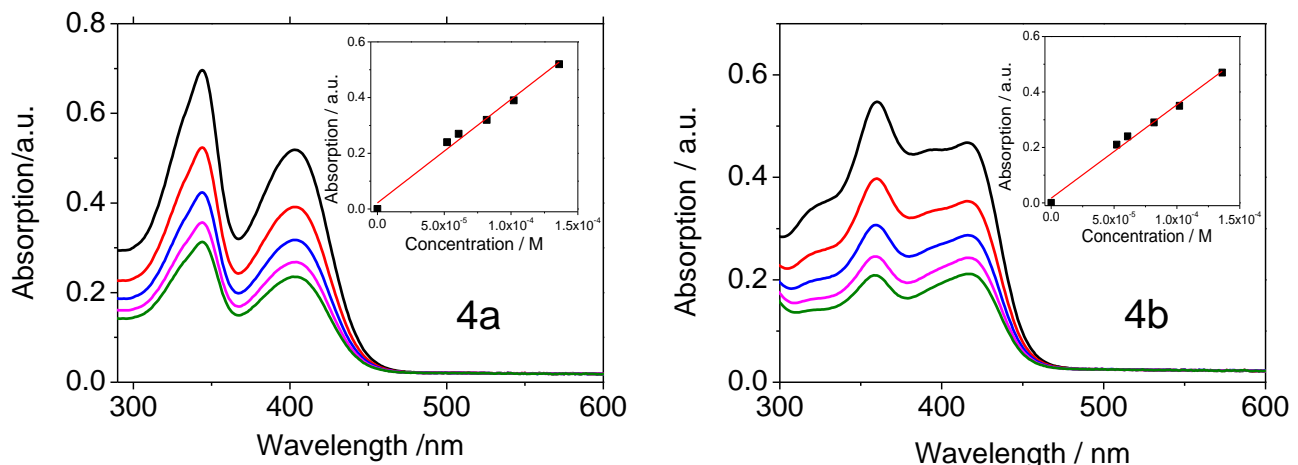
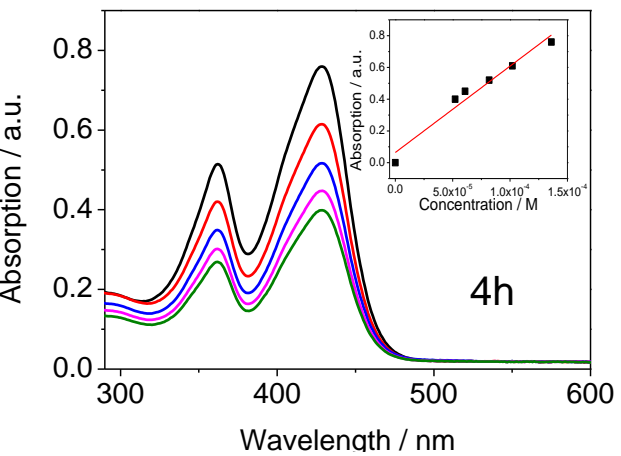
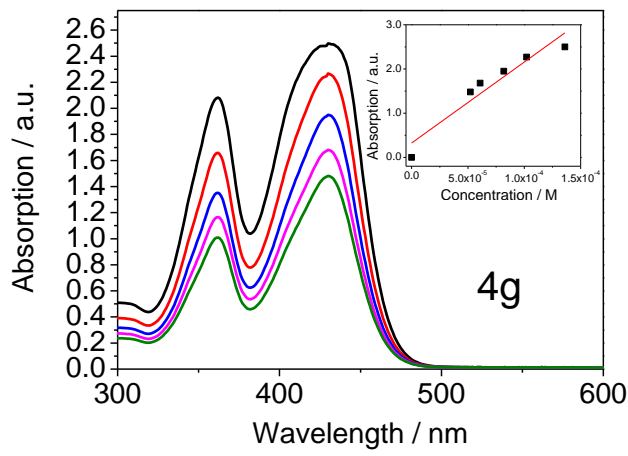
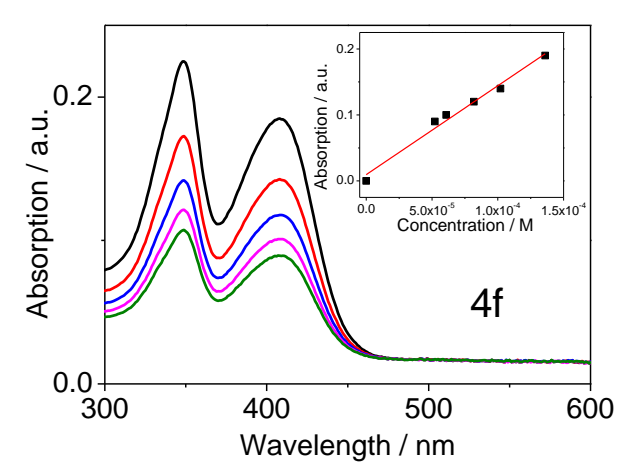
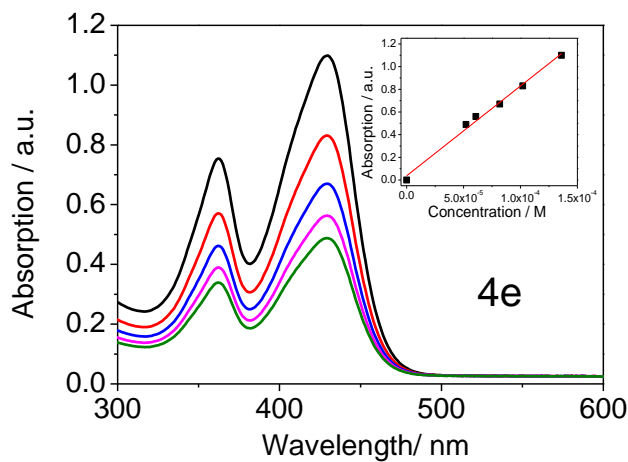
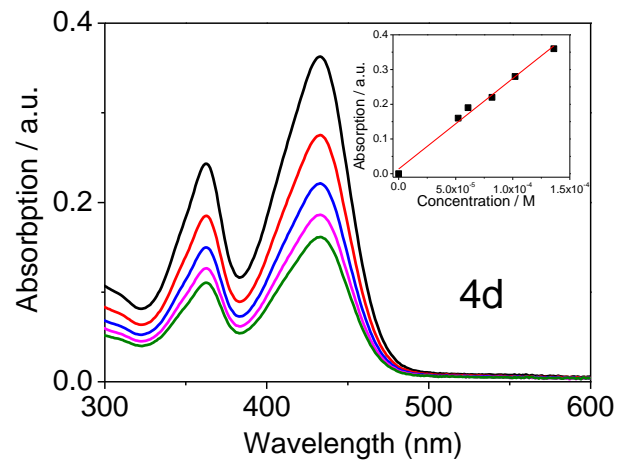
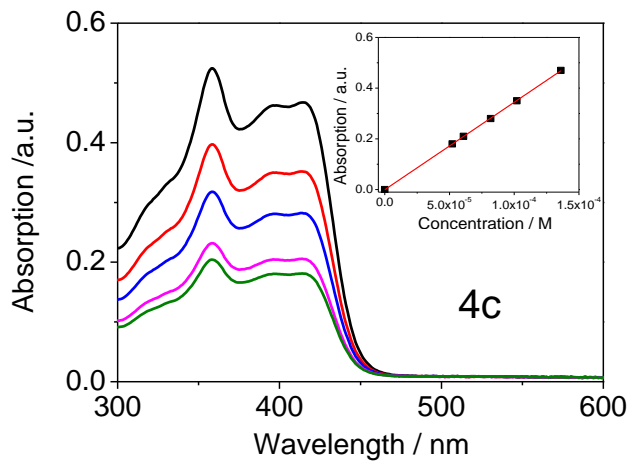


Figure 29S: Absorption spectra of the compounds in chloroform solution with concentration ranging from 5.0×10^{-5} to 1.0×10^{-4} M. Inset shows the maximum absorption intensities with concentration of the compound whereas the molar absorption coefficients (ϵ) of the compounds were evaluated from slopes of the curves using the Beer-Lambert law.





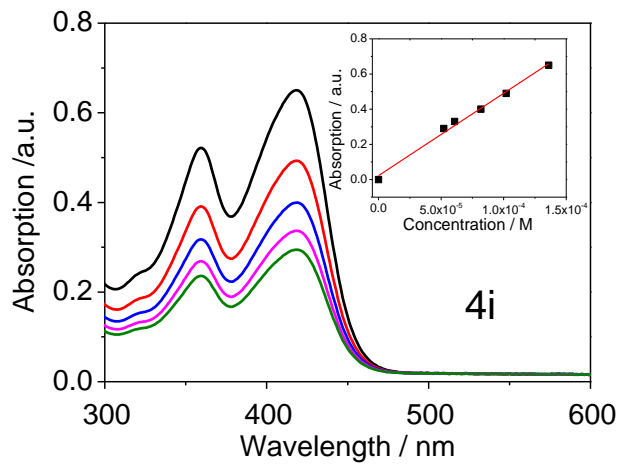
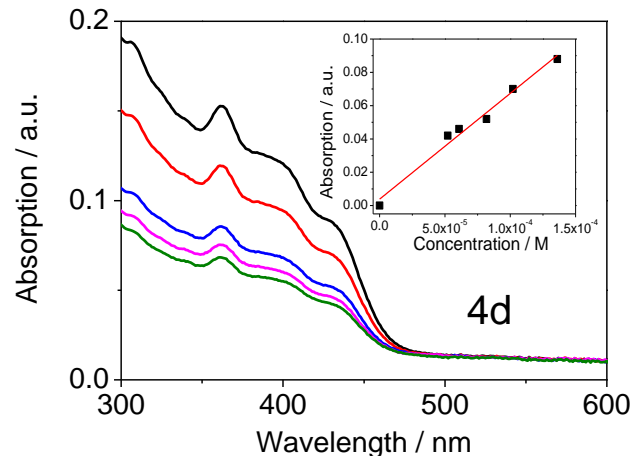
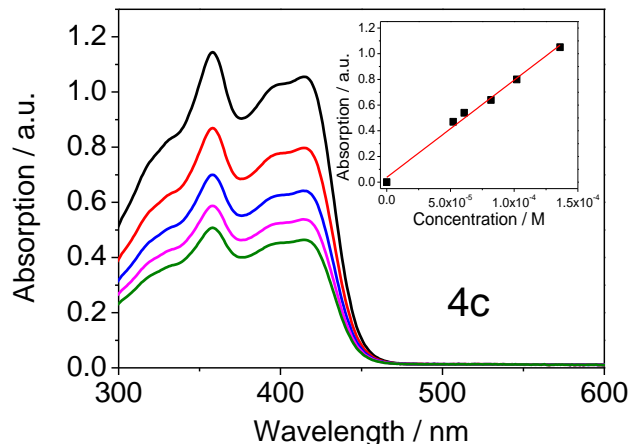
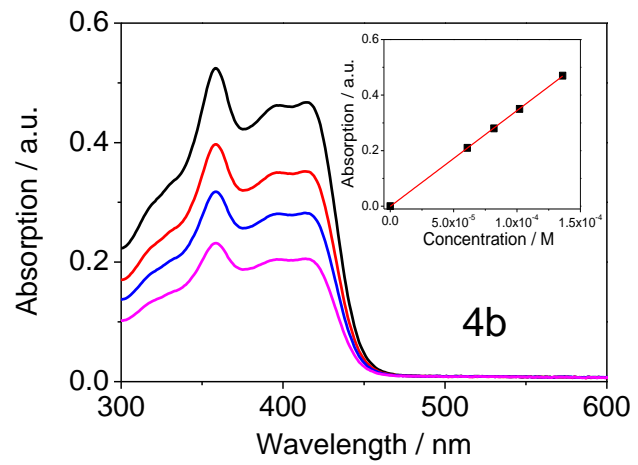
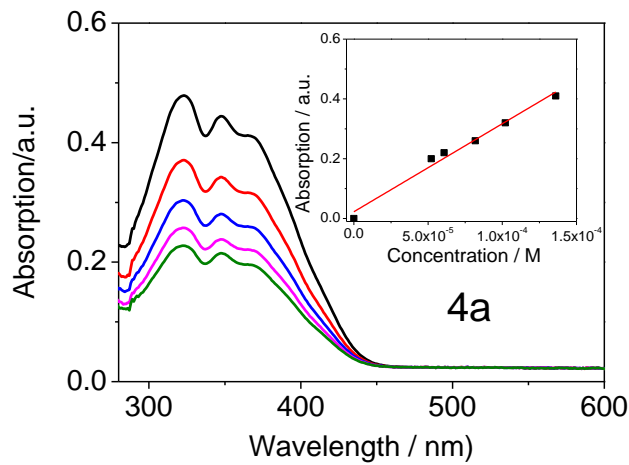


Figure 30S: Absorption spectra of the compounds in acetonitrile solution with concentration ranging from 5×10^{-5} to 1×10^{-4} M. Inset shows the maximum absorption intensities with concentration of the compound whereas the molar absorption coefficients (ϵ) of the compounds were evaluated from slopes of the curves using the Beer-Lambert law.



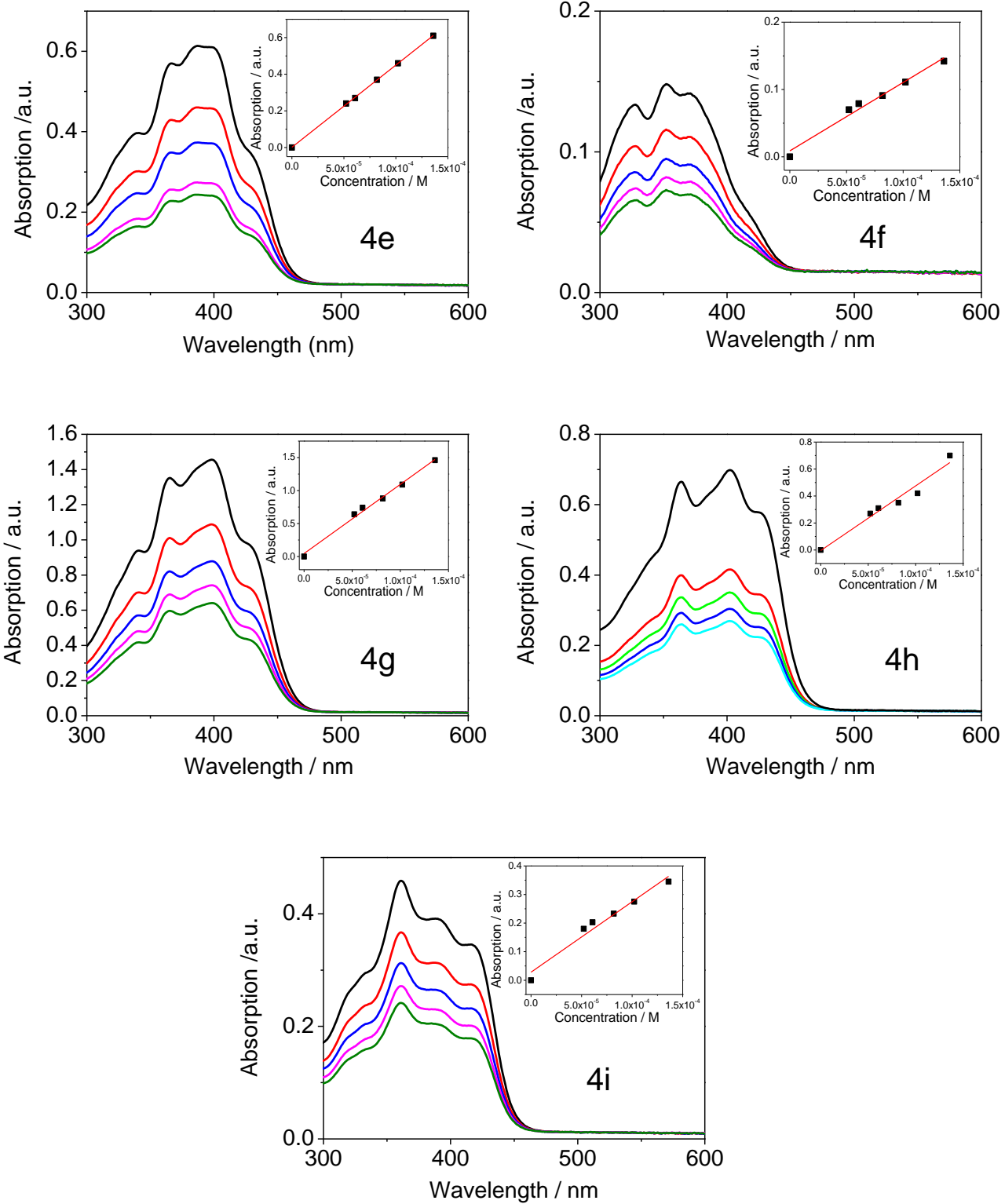


Figure 31S: Absorption spectra of the compounds in tetrahydrofuran solution with concentration ranging from 5×10^{-5} to 1×10^{-4} M. Inset shows the maximum absorption intensities with concentration of the compound whereas the molar absorption coefficients (ϵ) of the compounds were evaluated from slopes of the curves using the Beer-Lambert law.

Fluorescence Decay Curves

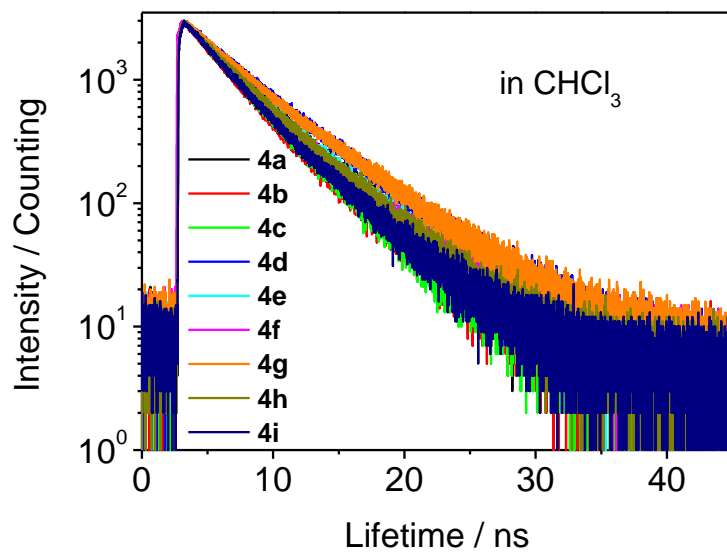


Figure 32S: The fluorescence decay curves of the compounds in chloroform solution

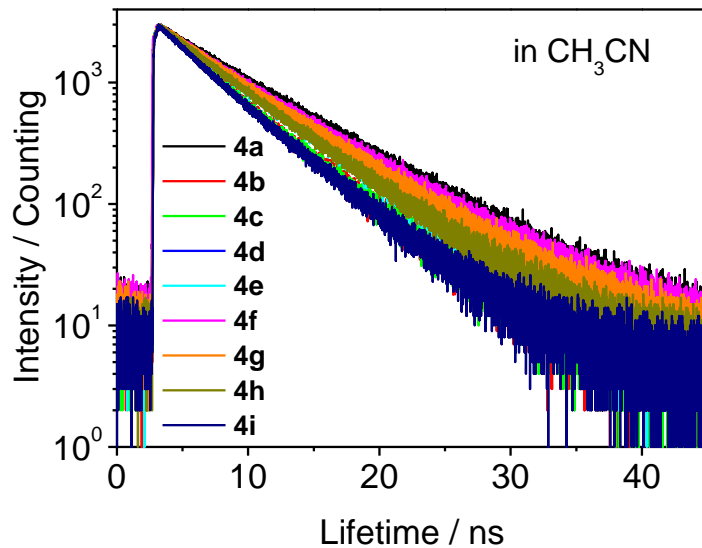


Figure 33S: The fluorescence decay curves of the compounds in acetonitrile solution

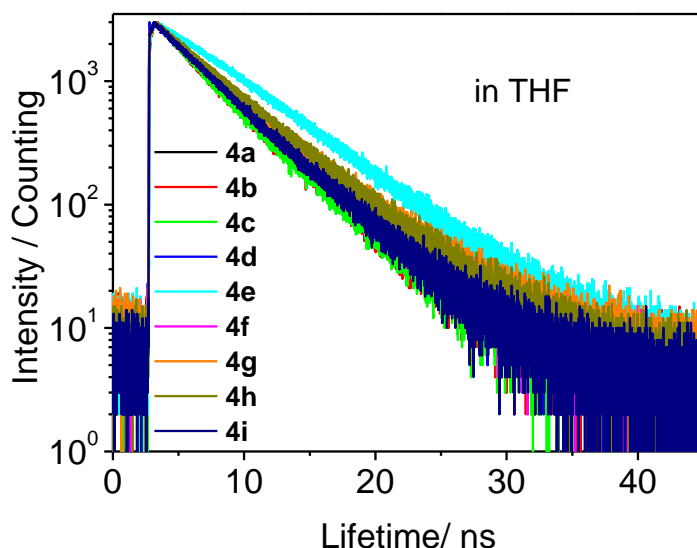


Figure 34S: The fluorescence decay curves of the compounds in tetrahydrofuran solution

Electrochemical properties of compounds: Cyclic voltammograms of the compounds 4a-i

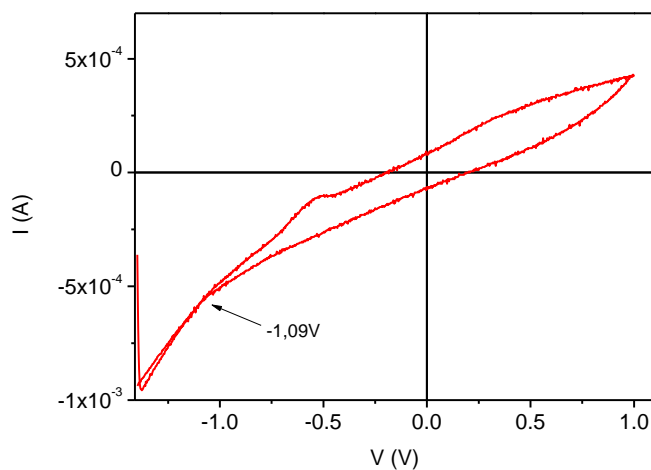


Figure 35S. Cyclic voltammograms of compound 4a

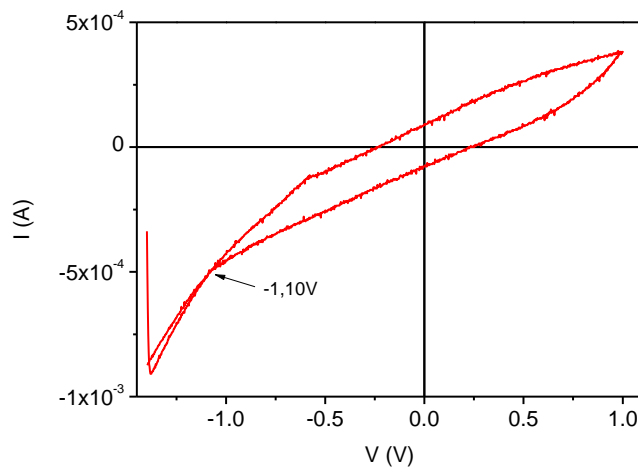


Figure 36S. Cyclic voltammograms of compound 4b

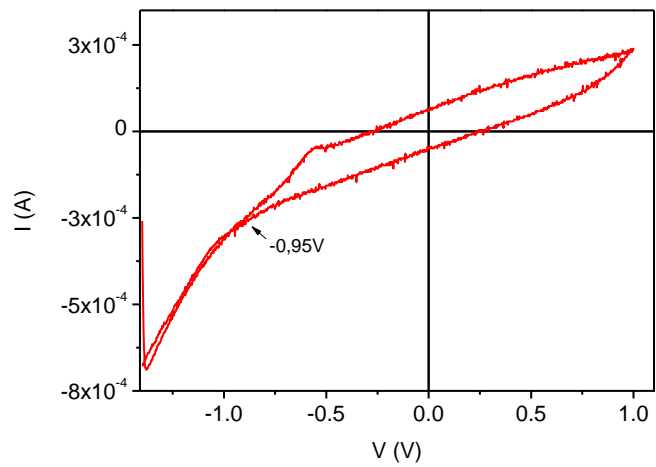


Figure 37S. Cyclic voltammograms of compound **4c**

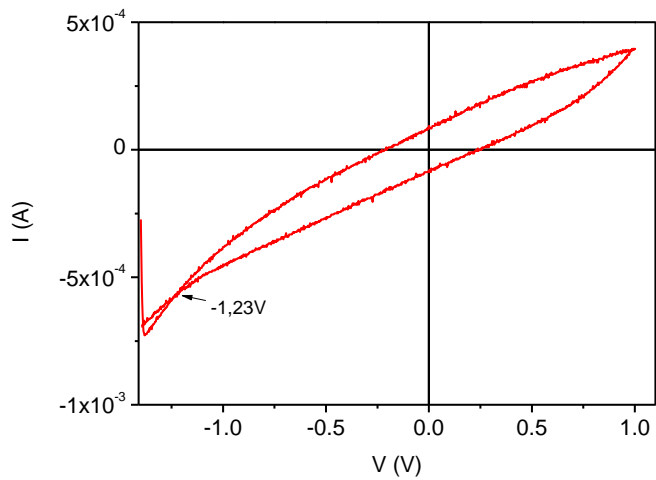


Figure 38S. Cyclic voltammograms of compound **4d**

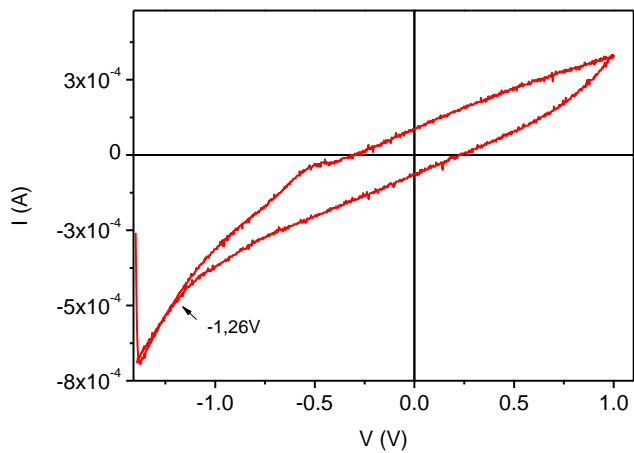


Figure 39S. Cyclic voltammograms of compound **4e**

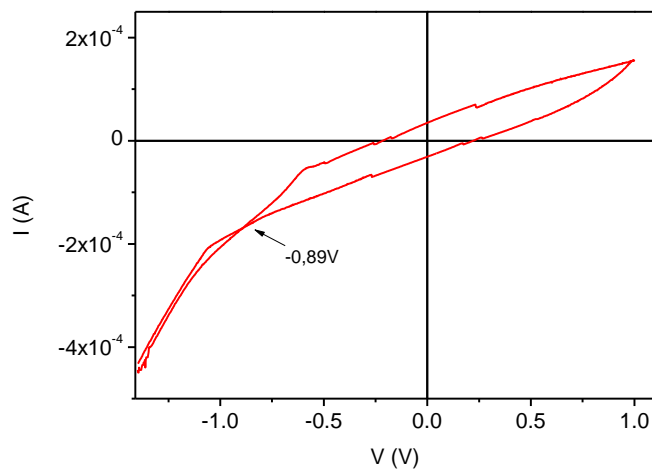


Figure 40S. Cyclic voltammograms of compound **4f**

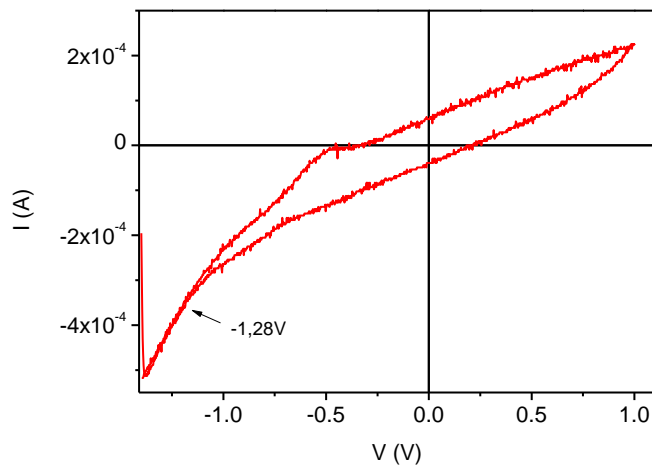


Figure 41S. Cyclic voltammograms of compound **4g**

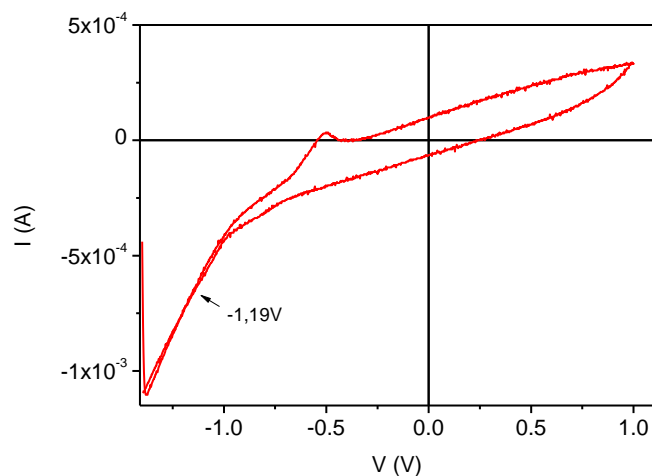


Figure 42S. Cyclic voltammograms of compound **4h**

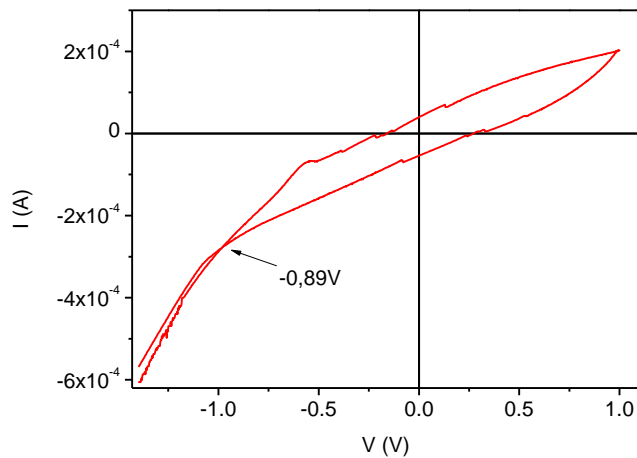


Figure 43S. Cyclic voltammograms of compound **4i**

Computational Studies for compounds **4a** and **4e**

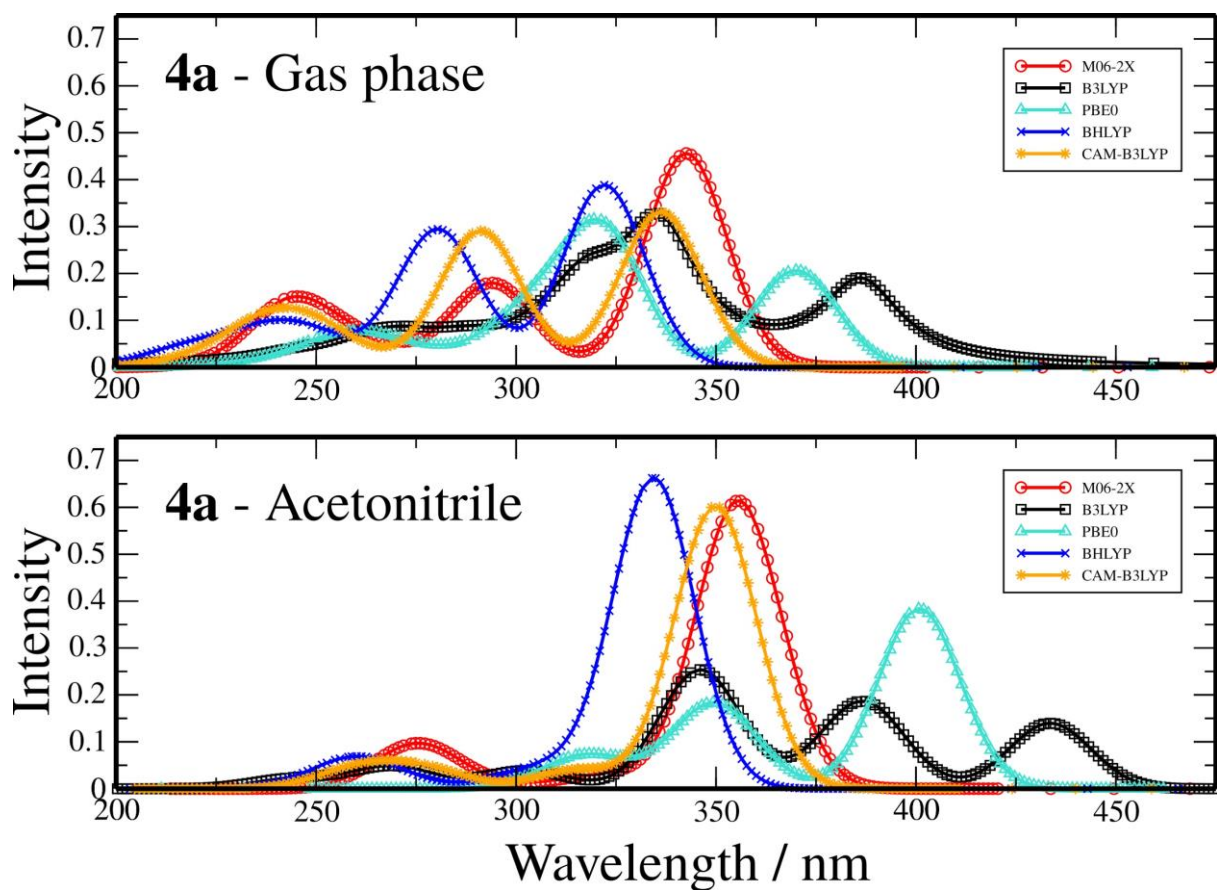


Figure 44S. Theoretical absorption spectra for 10 excited states for molecule **4a** compared for all exchange-correlation functionals studied for gas phase (top) and acetonitrile (down).

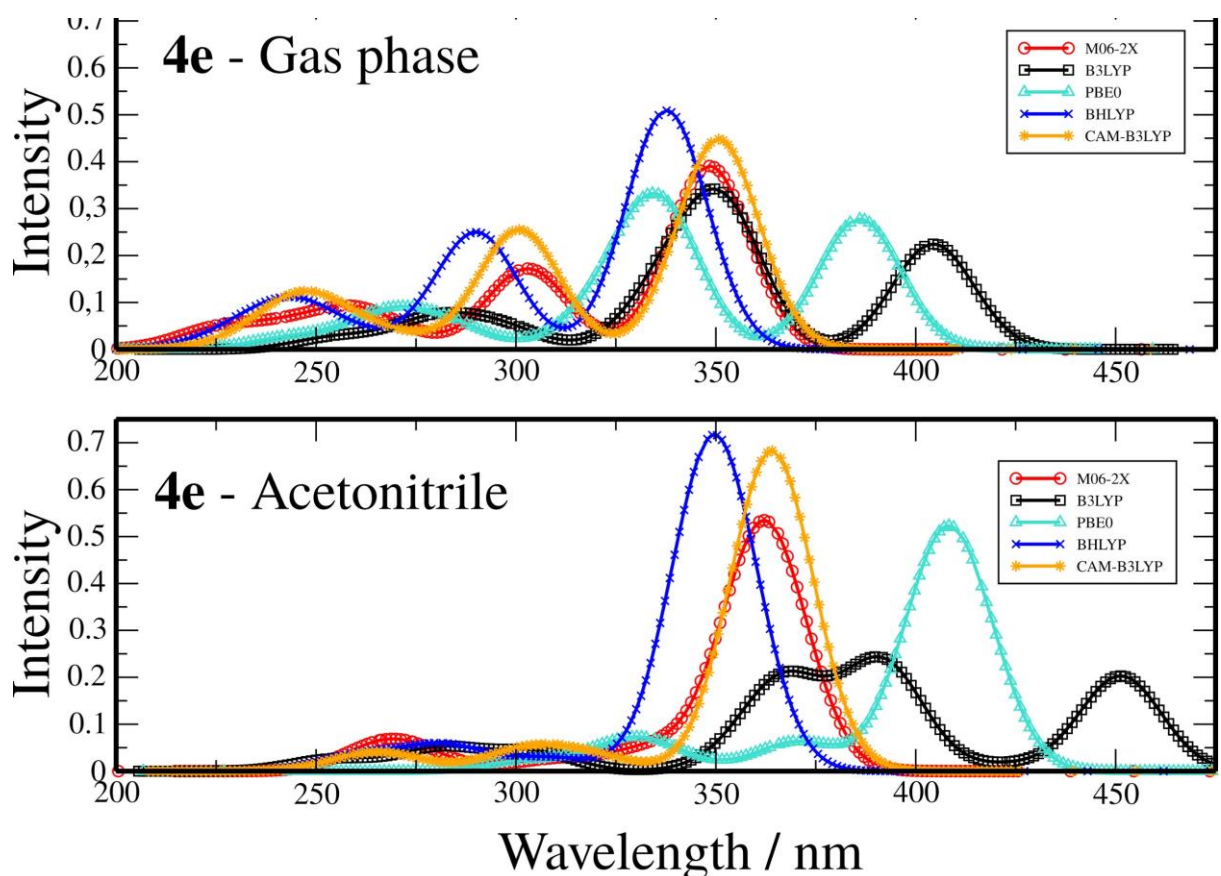


Figure 45S. Theoretical absorption spectra for 10 excited states for molecule 4e compared for all exchange-correlation functionals studied for gas phase (top) and acetonitrile (down).

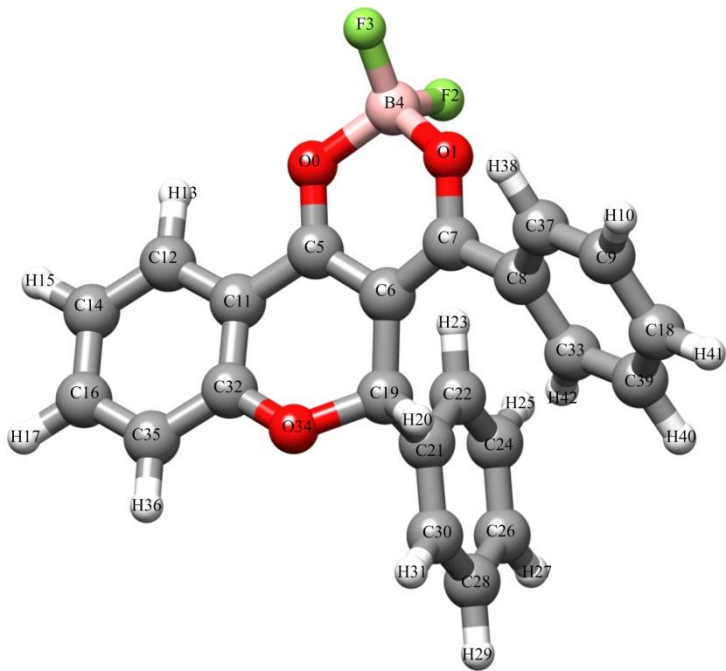


Figure 46S. Optimized geometry for molecule **4a**. Labels identify the atoms for the Table 3S.

Table 3S. Optimized Bond distances (\AA) and angles (degrees) selecting to molecule **4a**. Calculations were performed with DFT and B3LYP functional. Figure 44S shows the atom labels definition.

Bond	Distance (\AA)	Bond	Angle (°)	Bond	Angle (°)
B4-F2	1.3764	B4-O0-C5	121.15	C21-C22-H23	120.23
B4-O1	1.5083	B4-O1-C7	122.84	H23-C22-C24	119.29
B4-F3	1.3606	O1-B4-F2	108.48	C21-C22-C24	120.47
B4-O0	1.5116	O0-B4-F2	108.33	H25-C24-C26	120.22
C5-O0	1.2883	O1-B4-F3	109.00	C22-C24-C26	120.24
C6-C5	1.4085	F2-B4-F3	114.49	C22-C24-H25	119.54
C7-O1	1.2953	O0-B4-O1	107.32	H27-C26-C28	120.12
C7-C6	1.3995	O0-B4-F3	108.99	C24-C26-C28	119.68

C8-C7	1.4801	O0-C5-C11	117.55	C24-C26-H27	120.20
H10-C9	1.0829	C6-C5-C11	119.36	H29-C28-C30	119.87
C11-C5	1.4494	O0-C5-C6	122.93	C26-C28-C30	120.03
C12-C11	1.4035	C5-C6-C19	117.28	C26-C28-H29	120.09
H13-C12	1.0814	C5-C6-C7	117.36	C28-C30-H31	119.83
C14-C12	1.3805	C7-C6-C19	125.06	C21-C30-H31	119.45
H15-C14	1.0819	O1-C7-C8	113.76	C21-C30-C28	120.72
C16-C14	1.3991	C6-C7-C8	125.47	O34-C32-C35	118.13
H17-C16	1.0833	O1-C7-C6	120.66	C11-C32-C35	120.13
C18-C9	1.3923	C33-C8-C37	119.09	C11-C32-O34	121.65
C19-C6	1.5088	C7-C8-C37	117.97	C39-C33-H42	119.15
H20-C19	1.0881	C7-C8-C33	122.89	C8-C33-H42	120.54
C21-C19	1.5260	H10-C9-C18	120.13	C8-C33-C39	120.24
C22-C21	1.3928	C18-C9-C37	120.18	C19-O34-C32	117.31
H23-C22	1.0823	H10-C9-C37	119.69	C32-C35-H36	118.97
C24-C22	1.3931	C12-C11-C32	119.44	C16-C35-H36	121.61
H25-C24	1.0826	C5-C11-C32	118.08	C16-C35-C32	119.43
C26-C24	1.3880	C5-C11-C12	122.26	C9-C37-H38	120.42
H27-C26	1.0830	C11-C12-C14	120.35	C8-C37-H38	119.21
C28-C26	1.3930	C11-C12-H13	118.49	C8-C37-C9	120.38
H29-C28	1.0830	H13-C12-C14	121.16	C33-C39-H40	119.54
C30-C28	1.3869	H15-C14-C16	120.19	C18-C39-H40	120.20

C30-C21	1.3986	C12-C14- C16	119.56	C18-C39-C33	120.26
H31-C30	1.0837	C12-C14- H15	120.25		
C32-C11	1.4055	C14-C16- C35	121.07		
C33-C8	1.3986	C14-C16- H17	119.70		
O34-C32	1.3509	H17-C16- C35	119.23		
O34-C19	1.4561	C9-C18-H41	120.10		
C35-C32	1.3938	C9-C18-C39	119.82		
C35-C16	1.3850	C39-C18- H41	120.08		
H36-C35	1.0818	H20-C19- C21	108.57		
C37-C9	1.3858	C6-C19-C21	115.67		
C37-C8	1.4013	C6-C19-H20	109.54		
H38-C37	1.0814	C21-C19- O34	108.53		
C39-C33	1.3897	H20-C19- O34	102.36		
C39-C18	1.3895	C6-C19-O34	111.31		
H40-C39	1.0829	C19-C21- C22	123.10		
H41-C18	1.0830	C22-C21- C30	118.86		
H42-C33	1.0812	C19-C21- C30	118.05		

Table 4S. Optimized Bond distances (\AA) and angles (degrees) selecting to molecule **4e**. Calculations were performed with DFT and B3LYP functional. Figure 1 shows the atom labels definition.

Bond	Distance (\AA)	Bond	Angle ($^{\circ}$)
O(2)-C(3)	1.2895	C(3)-O(2)-B(1)	120.8167
O(1)-C(1)	1.3002	C(1)-O(1)-B(1)	123.2185
O(2)-B(1)	1.5085	F(1)-B(1)-F(2)	114.2471
O(1)-B(1)	1.5036	F(1)-B(1)-O(1)	109.0227
F(2)-B(1)	1.3784	F(2)-B(1)-O(1)	108.612
F(1)-B(1)	1.3613	F(1)-B(1)-O(2)	109.1807
C(3)-C(2)	1.4078	F(2)-B(1)-O(2)	108.2181
C(3)-C(4)	1.4498	O(1)-B(1)-O(2)	107.2642
C(2)-C(1)	1.404	O(2)-C(3)-C(2)	123.2112
C(2)-C(14)	1.5092	O(2)-C(3)-C(4)	117.1626
C(14)-C(15)	1.5254	C(2)-C(3)-C(4)	119.5437
C(10)-S(1)	1.7394	C(3)-C(2)-C(1)	117.5049
C(10)-C(11)	1.3828	C(3)-C(2)-C(14)	117.1401
C(12)-C(11)	1.4072	C(10)-S(1)-C(13)	92.1963
C(4)-C(9)	1.4041	C(4)-C(9)-O(3)	121.5088
C(4)-C(5)	1.4033	C(4)-C(9)-C(8)	120.2512

Table 5S. Excitations energies (in eV and nm), Oscillator Strength (fosc), and main orbitals electronic transition calculated with full TDDFT with B3LYP/def2-TZVP for molecule **4a**. In the transitions the orbitals 96 and 97 are the HOMO and LUMO, respectively.

State	Transition ($\geq 10\%$)	E / eV	λ / nm	fosc
1	96 → 97 (95%)	3.210	386.3	0.170809152
2	95 → 97 (93%)	3.693	335.7	0.273949741
3	94 → 97 (98%)	3.900	317.9	0.019052243
4	93 → 97 (95%)	3.914	316.8	0.117756096
6	91 → 97 (88%)	4.324	286.7	0.027901013
7	90 → 97 (88%)	4.558	272	0.033283194
9	96 → 98 (86%)	4.748	261.1	0.028003944
10	96 → 100 (80%)	5.073	244.4	0.013384248
12	95 → 98 (72%)	5.181	239.3	0.026443151
14	96 → 101 (68%) 96 → 102 (10%)	5.333	232.5	0.022971295
15	88 → 97 (13%) 94 → 98 (28%) 96 → 102 (23%)	5.448	227.6	0.049643849
17	88 → 97 (72%)	5.483	226.1	0.01321619
19	93 → 98 (34%)	5.590	221.8	0.036506356

	94 → 98 (28%)			
22	87 → 97 (36%) 95 → 101 (34%)	5.822	213	0.016565902
23	87 → 97 (13%) 91 → 98 (34%) 95 → 101 (13%)	5.859	211.6	0.038940285
24	87 → 97 (14%) 91 → 98 (14%) 93 → 100 (13%) 94 → 99 (12%)	5.911	209.8	0.076544986
26	86 → 97 (11%) 87 → 97 (12%) 94 → 99 (22%) 95 → 102 (16%) 96 → 103 (16%)	5.945	208.5	0.033539019
28	86 → 97 (11%) 93 → 99 (10%) 93 → 100 (13%) 94 → 99 (19%) 94 → 101 (15%)	6.015	206.1	0.034965853
29	92 → 100 (18%) 93 → 99	6.03	205.6	0.012450534

	(18%)			
30	82 → 97 (15%) 86 → 97 (31%) 90 → 98 (10%)	6.043	205.2	0.022034954

Table 6S. Excitations energies (in eV and nm), Oscillator Strength (fosc), and main orbitals electronic transition calculated with full TDDFT with B3LYP/def2-TZVP for molecule **4e**. In the transitions the orbitals 97 and 98 are the HOMO and LUMO, respectively.

State	Transition (≥10%)	E / eV	λ / nm	fosc
1	97 → 98 (93%)	3.066	404.4	0.224529310
2	96 → 98 (87%)	3.524	351.8	0.291237391
3	95 → 98 (86%)	3.671	337.7	0.105519184
4	94 → 98 (96%)	3.714	333.8	0.013623090
6	93 → 98 (20%) 92 → 98 (69%)	4.200	295.2	0.041282564
7	91 → 98 (45%) 97 → 99 (47%)	4.424	280.3	0.039450197
8	91 → 98 (50%) 97 → 99 (38%)	4.453	278.4	0.016901852
10	96 → 99 (85%)	4.870	254.6	0.024583897
12	94 → 99 (45%) 95 → 99 (29%) 97 → 100 (13%)	5.096	243.3	0.020891773
13	94 → 99 (18%) 95 → 99 (62%) 97 → 100 (10%)	5.131	241.6	0.023999761
14	97 → 101 (82%)	5.281	234.8	0.018171715
18	93 → 99 (46%) 93 → 99 (37%)	5.539	223.8	0.093964106

19	92 → 99 (49%) 93 → 99 (13%) 96 → 100 (20%)	5.572	222.5	0.046046646
20	91 → 99 (13%) 92 → 99 (16%) 96 → 100 (19%) 97 → 102 (16%)	5.656	219.2	0.016147459
22	91 → 99 (20%) 92 → 99 (10%) 96 → 101 (20%) 97 → 103 (24%)	5.770	214.9	0.012774448
23	91 → 99 (21%) 96 → 101 (12%) 97 → 103 (26%) 97 → 104 (16%)	5.819	213.1	0.026391595
24	91 → 99 (23%) 96 → 101 (26%) 96 → 102 (20%)	5.855	211.8	0.039512209
25	87 → 98 (58%) 97 → 104 (14%)	5.887	210.6	0.022891242
26	94 → 101 (15%) 95 → 100 (63%)	5.915	209.6	0.035918586
27	97 → 103 (20%) 97 → 104 (33%)	5.948	208.4	0.082427580
28	96 → 102 (44%)	5.965	207.9	0.105858928
29	86 → 98 (50%) 87 → 98 (16%)	5.986	207.1	0.017980533
30	95 → 101 (25%) 95 → 102 (45%)	6.113	202.8	0.019074172

Table 7S. Main excited states for molecules **4a** and **4e** and their respective oscillator strength values (f_{osc}) for different solvents calculated with B3LYP functional.

	State 1	f_{osc}	State 2	f_{osc}	State 3	f_{osc}	State 4	f_{osc}
Compound 4a								
gas phase	386.3	0.171	335.7	0.274	317.9	0.019	316.8	0.118

CH ₃ CN	433.6	0.139	387.3	0.174	420.0	0.002	346.0	0.253
CHCl ₃	432.3	0.142	379.8	0.198	427.0	0.002	346.3	0.220
THF	432.6	0.141	382.5	0.189	424.0	0.002	345.9	0.233
Compound 4e								
gas phase	404.4	0.225	351.8	0.291	337.7	0.106	333.8	0.014
CH ₃ CN	451.3	0.203	391.7	0.232	367.0	0.194	423.5	0.014
CHCl ₃	442.6	0.210	378.4	0.262	369.8	0.131	427.6	0.016
THF	451.5	0.236	388.4	0.281	367.3	0.193	432.2	0.016